



HAL
open science

Modeling Jamming Caused by Debris Flows Through a Series of Cascading Structures

Hilary Shirra

► **To cite this version:**

Hilary Shirra. Modeling Jamming Caused by Debris Flows Through a Series of Cascading Structures. Univ. Grenoble Alpes; Grenoble INP; ENSE3. 2024, pp.61. hal-04670924

HAL Id: hal-04670924

<https://hal.inrae.fr/hal-04670924v1>

Submitted on 28 Oct 2024

HAL is a multi-disciplinary open access archive for the deposit and dissemination of scientific research documents, whether they are published or not. The documents may come from teaching and research institutions in France or abroad, or from public or private research centers.

L'archive ouverte pluridisciplinaire **HAL**, est destinée au dépôt et à la diffusion de documents scientifiques de niveau recherche, publiés ou non, émanant des établissements d'enseignement et de recherche français ou étrangers, des laboratoires publics ou privés.



Distributed under a Creative Commons Attribution 4.0 International License

Modeling Jamming Caused by Debris Flows Through a Series of Cascading Structures

Hilary Shirra^{1,2}

¹*Univ. Grenoble Alpes, INRAE, CNRS, IRD, Grenoble INP, IGE, 38000 Grenoble, France*

²*BGC Engineering, Vancouver, BC, Canada*



**MINISTÈRE
DE LA TRANSITION
ÉCOLOGIQUE
ET DE LA COHÉSION
DES TERRITOIRES**

*Liberté
Égalité
Fraternité*

Funding: This work was funded by the French ministry of ecology (MTECT) under the 2024 joint agreement between INRAE and the DGPR service (Action: *DFbuffering*).

Citation: Shirra, H. 2024. *Modeling Jamming Caused by Debris Flows Through a Series of Cascading Structures* [Msc Thesis] Univ. Grenoble Alpes, Grenoble-INP, ENSE³, 61 pp. <https://hal.inrae.fr/hal-04670924>

Abstract

Debris flows are a hazard present in many mountain regions. They typically occur when steep mountain creeks flood, transporting sediment, woody debris, and often large boulders. Large boulders can cause jamming through constrictions during debris flow events, affecting the outflow rate of the debris flow, and causing sediment deposition. In 2022, Piton et al. developed a model to possibilistically simulate boulder jamming in a debris basin, and its effects on multi-phase flow. The Piton et al. (2022, *Journal of Geophysical Research*, DOI: 10.1029/2021JF006447) model uses simple hydraulic equations, basic geometry, and stochastic generation of boulders to simulate jamming. The possibilistic nature of the model allows it to encompass the uncertainty associated with the simulation of debris flows through uncertainty propagation.

In this study, we present an extension to the Piton et al. (2022) framework, wherein jamming can be possibilistically simulated through a series of debris basins or bridges (previously, the Piton et al. (2022) model was only able to simulate jamming through a single debris basin). The updated framework is able to route the event hydrograph between consecutive structures and can either route stochastically generated boulders directly to the downstream structure or regenerate boulders if deposition/erosion (i.e. "mixing") is expected between consecutive structures. The model framework is freely available through an online interface at <https://platrisk.ige.inrae.fr>. The code is open source and available on GitHub where it can be downloaded for R.

The updated framework was used to simulate the Torrent du Saint-Martin, a steep creek within the Maurienne Valley, France. The input parameters used to simulate jamming within the Torrent du Saint-Martin were measured, researched, or estimated using a variety of methods. Two simulations were conducted: a re-creation of the June 2005 event (a historical debris flow event that occurred along the Torrent du Saint-Martin) to compare the results of the updated framework against a known historical event, exploring the validity of the approach; and a parametric analysis to assess the monotony of the input variables and the model's sensitivity.

The results of the simulation of the 2005 event aligned with the historical records. The simulated jamming height and deposited debris flow volume upstream of the modeled structures aligned with the historical records of the debris flow. The results of the parametric analysis also aligned with expectations. The simulated monotony of the input variables were consistent with expected debris flow behavior and were added to the framework to reduce model runtime. Most model inputs (with the exception of event volume and peak inflow) had a minor impact on the model results, varying the outflow volume and peak outflow by 15% or less, indicating that the model is robust in the face of uncertainty. Overall, the results of the analyses indicate that the model can be effectively used to simulate jamming caused by a debris flow through a series of debris basins or bridges.

Contents

Notations	iv
1 Introduction	1
2 Materials and Methods	3
2.1 Torrent du Saint-Martin	3
2.1.1 Watershed Description	3
2.1.2 Existing Mitigations	4
2.1.3 History of Debris Flows	6
2.2 Modeling Framework	7
2.2.1 Summary of Piton et al. (2022) Framework	7
2.2.2 Extension of Piton et al. (2022) Framework to a Series of Constrictions	10
2.2.3 Plain Language Summary of Framework	14
2.3 Case Study Procedure	16
2.3.1 2005 Event	16
2.3.2 Parametric Analysis	22
3 Results	22
3.1 Definition of Final Input Parameters	22
3.2 2005 Event	24
3.3 Parametric Analysis	27
4 Discussion	30
4.1 2005 Event	30
4.2 Parametric Analysis	31
4.3 Limitations and Future Directions	31
5 Conclusion	31
References	i
A Structural Mitigations of the Torrent du Saint-Martin	i
B General Updates to Model Framework	i
C Input Parameters	i
D Methodology for Volume-Elevation Curve Development	i
E Model Results	i
F Limitations and Future Directions	i

Notations

$\langle n_j \rangle$	The mean number of boulders of class j within a reference volume V_{ref}
Δt	Time step of computation [s]
Δt_{mix}	Duration it took before time step i to discharge a total volume V_{mix} [s]
μ	Weir or orifice coefficient [-]
ϕ	Angle of weir wing [°]
a_i	Height of the orifice [m]
D_j	Average diameter of a boulder within class- j [m]
i	The index of the openings, starting at 1 from the bottom one
j	The index of the boulder class, starting at 1 from the biggest size
n	The index of a structure, starting at 1 from the most upstream
N_b	Number of boulders that pass a given point within the mixing volume
N_j	Number of packets of boulders of class- j
n_j	Number of boulders of class- j counted in a given volume
p_j	The probability of a boulder of class j existing within a packet
Q_{in}	Discharge at a structure inlet [m^3]
Q_{out}	Discharge at a structure outlet [m^3]
S	Channel slope upstream of a bridge [m/m]
S_{dep}	Deposition slope of the debris flow upstream of a constriction [m/m]
V	Storage within a structure [m^3]
V_j	Average boulder volume within class- j [m^3]
$V_{control}$	Total volume of debris flow passing through the constriction at time t [m^3]
V_{mix}	Mixing volume for boulder transfer between two subsequent structures [m^3]
V_{ref}	A reference volume of debris flow on which a counting of boulder is performed [m^3]
w_0	Mean width of the rectangular equivalent of the channel upstream a bridge [m]
$w_i(t)$	Opening width [m]
$y_i(t)$	Vertical distance between the base of the opening and the boulder jam upper level [m]

1 Introduction

Debris flows are a hazard present in many mountain regions (Xiong et al., 2016). They typically occur when steep mountain creeks flood, transporting sediment, woody debris, and often large boulders (Piton and Recking, 2016). If not properly managed, debris flows can pose serious economic or life-loss risk (Xiong et al., 2016).

Mitigation measures can be constructed within the catchments of steep mountain creeks to reduce debris flow hazard. There are a variety of well-documented mitigation strategies including diversion, hillslope buttressing, channel stabilization, soil conservation, transformation, wood filtration, debris buffering, debris deposition, water retention, and conveyance (Piton et al., 2024). The effectiveness of some of these mitigation strategies (such as conveyance) is reduced by channel blockage. Conversely, some mitigation strategies (such as deposition and transformation) are reliant on partial or complete blockage of the channel during a debris flow event (Piton et al., 2024). For example, open check dams and sabo dams (hereafter collectively referred to as debris basins), are often designed to either constrict flow (encouraging upstream deposition) or to block the passage of large boulders, while still allowing the flow of smaller sediment and water (Piton et al., 2024). When assessing debris flow hazard, or designing a mitigation, it is therefore important to be able to accurately predict jamming (Piton et al., 2022).

Jamming is more likely to occur in channel constrictions, both natural and man-made. Constrictions impact flow, and can cause sediment deposition through two main mechanisms (Piton et al., 2022):

1. Hydraulic control, in which the constriction causes backwatering to occur, reducing shear stress and therefore sediment transport capacity.
2. Mechanical control, in which the constriction becomes blocked with debris too coarse to pass through, inhibiting the passage of sediment.

Jamming can be caused either by one boulder with a diameter greater than the constriction or by two or more boulders with a combined diameter larger than the constriction width, arriving at the constriction together (Piton et al., 2022). Jamming may also occur when three or more particles form arches (Marchelli et al., 2020), but such granular formations are unstable. Examples of jamming are shown in Figure 1.



Figure 1: Examples of boulder jamming from debris flows in the French Alps. Figure taken from Piton *et al.* (2022).

It is generally accepted that if the opening of a constriction is 3 times larger than the diameter of the coarsest particles in a debris flow, jamming is unlikely, and if the opening is only 1.5 times larger than the diameter of the coarsest particles, then jamming is likely (Piton and Recking, 2016). Even with these guidelines, however, it is difficult to accurately predict jamming, due to the inherent randomness in the shape, size, and distribution of large boulders within a debris flow event. In 2022, Piton *et al.* developed a model that can stochastically evaluate boulder jamming through constrictions (Piton *et al.*, 2022).

Before the development of the Piton *et al.* (2022) model, jamming could only be explicitly evaluated through fluid mechanic solvers (e.g. Canelas *et al.*, 2017; Nakatani *et al.*, 2016), or estimated using back-of-the-envelope calculations (i.e. using the ratio of opening size to particle diameter to estimate whether jamming is likely. With this methodology, however, the height of the jam remains unknown, which is an issue for high barriers Piton and Recking, 2016). While useful, explicit modeling is unable to address the stochastic nature of jamming, as model run times are too high to propagate the requisite uncertainty effectively (Canelas *et al.*, 2017). Back-of-the-envelope calculations are fast but fuzzy, and they cannot be used to predict attenuation due to jamming, which is an important design consideration. For these reasons, these jamming prediction methodologies are insufficient for many design applications.

The Piton *et al.* (2022) model (which will be described in more detail in Section 2.2) is able to stochastically simulate jamming in debris basins, and its effects on multi-phase flow. However, the Piton *et al.* (2022) model was only able to evaluate one constriction and not multiple constrictions in series. Barbini *et al.* (2024) addressed this problem by integrating the Piton *et al.* (2022) model into the Gregoretto *et al.* (2019) hydraulic model, modified by Bernard and Gregoretto (2021), to simulate debris flow jamming through a series of constrictions. The purpose of the Barbini *et al.* (2024) model was to validate a debris flow mitigation design for a steep creek in Italy. While the Barbini *et al.* (2024) model is able to simulate jamming through a series of constrictions, it is a fluid mechanic solver and therefore faces the same problem as other explicit models - an inability to stochastically simulate jamming due to time and computational power constraints.

In this study, the Piton *et al.* (2022) framework was extended to be able to possibilistically model jamming through a series of constrictions in the form of debris basins or bridges. This is relevant

when assessing the effectiveness of, for example, a cascading series of debris basins, or several bridges passing over a channel. This extended framework is presented in this study, and its effectiveness is tested at a candidate site: the Torrent du Saint-Martin.

2 Materials and Methods

2.1 Torrent du Saint-Martin

2.1.1 Watershed Description

The Torrent du Saint-Martin is located north of the community of Saint-Martin-de-la-Porte within the Maurienne Valley, France (ONF-RTM, 2013). Its watershed has an area of 19km^2 , with a maximum altitude of 2825 m, and a minimum altitude of 680 m. There are multiple channels within the watershed. The two main tributaries (Ruisseau Benoît and Ruisseau de Bonrieu) converge at an altitude of 1010 m, before flowing into the Arc River. The longest channel has a continuous length of 7.7 km (ONF-RTM, 2023). An overview of the Torrent du Saint-Martin is shown in Figure 2.

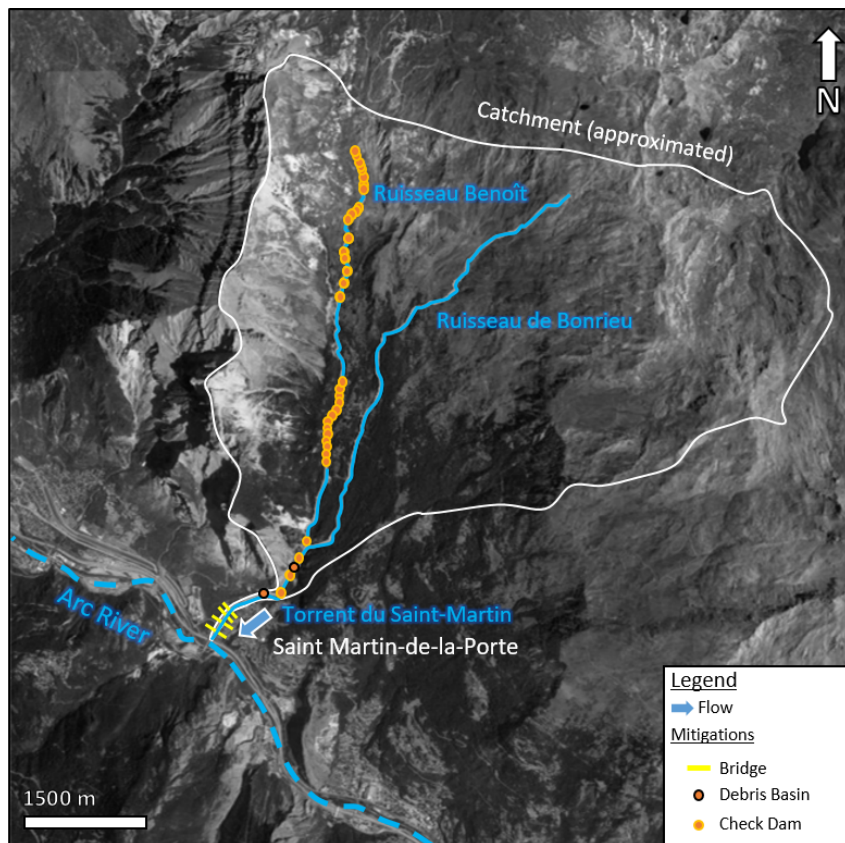


Figure 2: Overview of the Torrent du Saint-Martin watershed. Although there are many tributaries to the Torrent du Saint-Martin, only the two main ones (Ruisseau Benoît and Ruisseau de Bonrieu) are shown. The location and type of man-made constrictions within the channel are from (ONF-RTM, 2013, 2023; Hugerot, 2016). The catchment area and streamlines area are visually approximated from imagery. Background imagery from Google Earth (2022).

The upper watershed is sparsely vegetated in comparison to the lower watershed, making it prone to erosion, especially because its geology is made of weak rock types (including scree, schist, and liasic

limestone ONF-RTM, 2013). The basin is steep (0.24 m/m longitudinally, and 0.48 m/m transversally), leading to slope instability which supplies the channel with solid materials for transport. The channel is also steep, with an average slope of 0.21 m/m (ONF-RTM, 2023). These conditions make the Torrent du Saint-Martin prone to debris flow activity.

ONF-RTM (2013) used a variety of methods to estimate the frequency and magnitude of debris flows along the Torrent du Saint-Martin. These methods include an empirical analysis (i.e. using empirical equations to relate catchment parameters to event volume), a regional analysis (i.e. scaling frequency-magnitude relationships from nearby creeks to the Torrent du Saint-Martin watershed), a geomorphological analysis (i.e. estimating event volume based on debris availability within the watershed), and a historical analysis (based on historical events). These estimates, as well as the best estimate values, as determined by ONF-RTM (2013), are shown in Table 1. Details of the methodologies are available in ONF-RTM (2013).

Table 1: Frequency-magnitude relationship of debris flows along the Torrent du Saint-Martin, as estimated using various methodologies by ONF-RTM (2013). These ranges informed the event volumes selected for modeling.

Return Period (years)	10 (Frequent)	100 (Rare)	>100 (Exceptional)
Estimation method	Range of volume (m³)		
Empirical Evaluation	-	37 000 - 150 000	70 000 - 210 000
Regional Evaluation	9 000 -36 000	24 000 - 96 000	-
Geomorphological Evaluation	-	-	110 000
Historical Evaluation	33 000	44 000 - 92 000	-
Best Estimates	30 000	80 000	150 000

2.1.2 Existing Mitigations

Starting in 1880, extensive mitigation works have been constructed within the Torrent du Saint-Martin watershed, both inside and outside of the alluvial fan. Because of this, smaller, frequently occurring debris flow events do not usually damage nearby infrastructure (ONF-RTM, 2013). For the purposes of this study, modeling is limited to the structures within the alluvial fan. Mitigations outside of the fan are discussed in Appendix A

Mitigations Within the Alluvial Fan On the alluvial fan of the Torrent du Saint-Martin, there are five constrictions (Figure 3). These constrictions were visually inspected during a May 2024 site visit. The Upper Debris Basin and the Lower Debris Basin are check dams with an upstream debris basin. The Upper Debris Basin was originally constructed in 1986. It is actively maintained by the Service de Restauration des Terrains de Montagne (RTM), and was last repaired in 2012 (ONF-RTM, 2013). As part of the active maintenance, the structure has been progressively optimized in response to debris flow events. For example, in 2012 wings were added to guide flows above the slit during high flow conditions. The Upper Debris Basin was originally constructed with a grill, but when the grill was destroyed by a debris flow in 1993, the debris basin itself was observed to be able to effectively trap large boulders while still allowing routine events to pass, reducing maintenance costs (Carladous et al., 2022), and so the grill was not replaced. The Lower Debris Basin was constructed in 1995 (ONF-RTM, 2013). The RTM does not have any information on the maintenance of this structure (ONF-RTM, 2013), but it appeared to be in good condition during a May 2024 site visit. Downstream of the Lower Debris Basin, the Torrent du Saint-Martin channel is artificially straightened and armored. This channelization effort began in 1892 and is actively maintained (ONF-RTM, 2013). The Upper Bridge, Second Bridge, and Lower Bridge all pass over the channel.

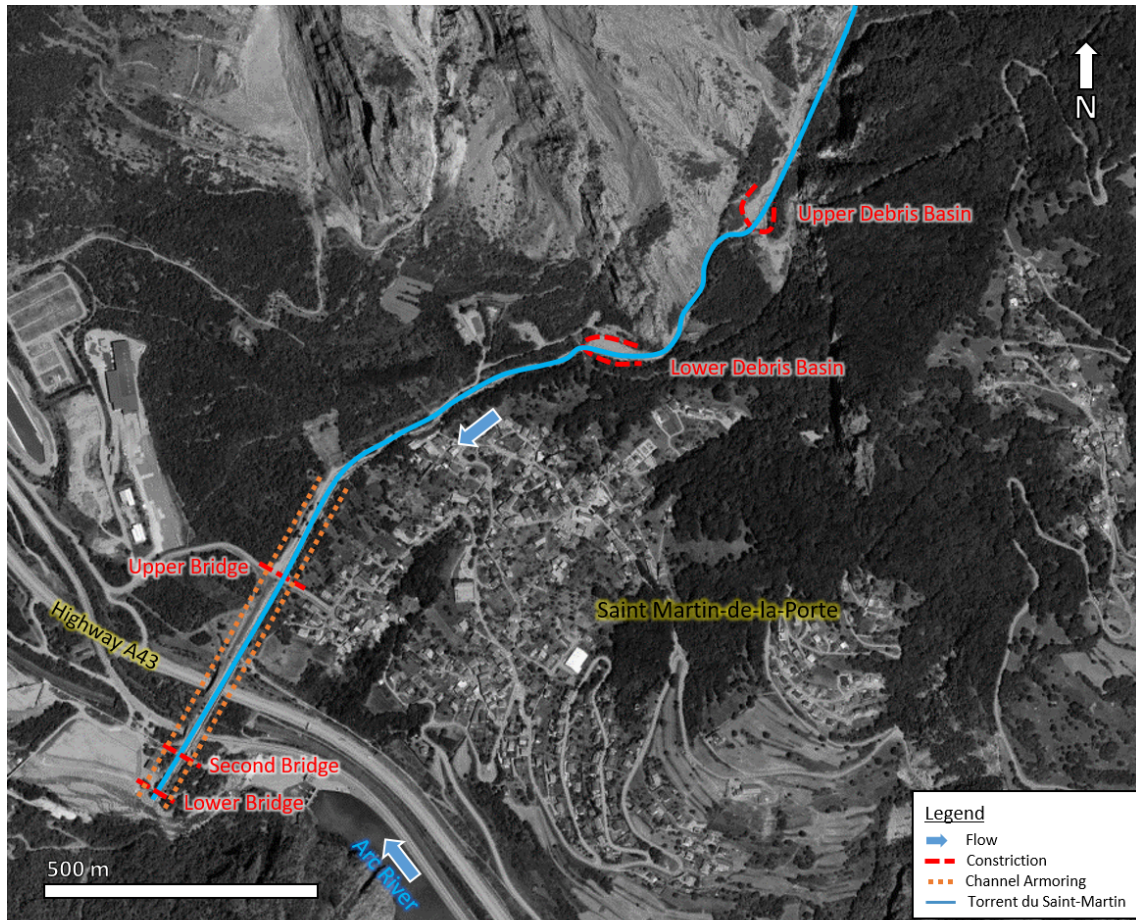


Figure 3: Constrictions within the alluvial fan of the Torrent du Saint-Martin (ONF-RTM, 2013). Background imagery: Esri World Imagery.

Because there is little infrastructure downstream of Highway A43, debris flow behavior in this section is less critical from a risk perspective. Smaller debris flow events may even completely deposit upstream of Highway A43 and the Upper bridge has the most restrained section of the three bridges. Therefore, only the three constrictions upstream of Highway A43 (the Upper Basin, the Lower Basin, and the Upper Bridge - Figure 3) were included in the model. These structures are shown in Figure 4.



Figure 4: Constrictions within the alluvial fan of the Torrent du Saint-Martin included in the model. The Upper Debris Basin is shown in panel a), the Lower Debris Basin in panel b), and the Upper Bridge in panel c). Photos from Carlados et al., 2022.

2.1.3 History of Debris Flows

Frequency of debris flow activity The Torrent du Saint-Martin is geomorphically active, with a record of 41 events dating back to the early 1400s. Most events have occurred as a result of summer thunderstorms, with 78% of recorded events occurring between the months of June and September (ONF-RTM, 2013). These events occur frequently and have the capacity to be destructive. In 1435, and again in 1649, flooding of the Torrent du Saint-Martin destroyed the hamlet of Plan Butin. Between 1776 and 2011, the Torrent du Saint-Martin had an average event frequency of one debris flow every 6.7 years. Between 2000 and 2011, 5 events were recorded (an average of one every 2.2 years), indicating that event frequency may be increasing with time (ONF-RTM, 2013).

Routine events Typical routine events in the Torrent du Saint-Martin tend to pass through the wide slit of the debris basins with marginal side deposit, and to be conveyed through the lined channel also with marginal deposit and without overflowing. Such events might have a non-negligible volume, possibly of a few thousand m^3 . The steep and continuous nature of the channel and the room available at the confluence make these events non-damaging, save for minor levee deposits at the tip of the channel bank.

The 2005 Event The most destructive debris flow event along the Torrent du Saint-Martin since 1649, occurred on June 22, 2005. The event was categorized as "exceptional", corresponding to an event return period of greater than 100 years, and a best estimate event volume of 150 000 m^3 (Table 1). Eyewitnesses say that the event came in two surges. Although it lasted less than 20 minutes, the 2005 event washed away two bridges and damaged several more. Several mitigations were also damaged, including 6 check dams upstream of the alluvial fan, and channel armoring within the alluvial fan. 18 500 m^3 of debris was deposited in the Upper Debris Basin, and 5000 m^3 was deposited in the Lower Debris Basin. The 2005 debris flow partially jammed the Upper Debris Basin (Figure 5) (ONF-RTM, 2013), but we were unable to find any record of the Lower Debris Basin experiencing jamming, or failure during this event. We therefore assumed that the Lower Debris Basin was not jammed. The Upper Bridge was one of the two bridges washed away during the 2005 event, although we were unable to find historical records specifying whether this was due to jamming or simply overtopping. Because of this uncertainty and lack of record, we assumed that storage in the reach upstream of the Upper Bridge was negligible.

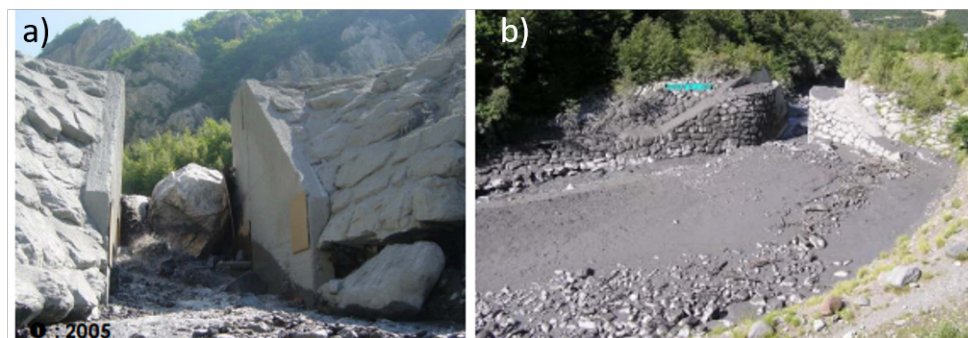


Figure 5: Looking upstream at boulders jamming the Upper Debris Basin following the June 2005 flood (a). Looking downstream at deposition within the Upper Debris Basin following the June 2005 flood (b). Photos from ONF-RTM, 2013.

2.2 Modeling Framework

2.2.1 Summary of Piton et al. (2022) Framework

Physics-based modeling In the Piton et al. (2022) model, a novel framework for analyzing boulder jamming during debris flows was developed. It is computationally light and combines well-established principles of statistical prediction, and fluid mechanics. It allows practitioners to possibilistically analyze (possibilities are an alternative method to probabilities to study uncertainty propagation) the effects of boulder-laden flows through a constriction for a large range of input parameters. In the Piton et al. (2022) paper, it was used to size the opening of the Cheekye Slit-Dam in Squamish, Canada. This framework is discussed in detail in Piton et al. (2022), and is summarized here.

For each time step (t), the Piton et al. (2022) model runs through the following steps:

1. Calculate the volume and depth of fluid in the basin upstream of the constriction based on the inflow hydrograph and the outflow from the constriction using hydraulics equations (1, 2, 3) and conservation of mass principals (4).
2. Stochastically generate boulders within the volume of debris flow currently passing through the constriction, and model jamming. If required, update the geometry of the constriction to account for jamming.

This routine is repeated until the hydrograph is complete. Each step within the routine is expanded upon below.

The hydraulics of the basin are calculated using either the slit equation (Eq 1), the grand orifice equation (Eq 2), or the weir equation (Eq 3). An equation is selected depending on the configuration of the opening(s).

$$Q_i(t) = \mu \cdot \frac{2}{3} \cdot \sqrt{2g} \cdot w_i(t) \cdot [h(t) - y_i(t)]^{3/2} \quad (1)$$

$$Q_i(t) = \mu \cdot \frac{2}{3} \cdot \sqrt{2g} \cdot w_i(t) \cdot [[h(t) - y_i(t)]^{3/2} - [h(t) - y_i(t) - a_i]^{3/2}] \quad (2)$$

$$Q_i(t) = \mu \cdot \frac{2}{3} \sqrt{2g} \cdot [w_i(t) \cdot [h(t) - y_i(t)]^{3/2} + \frac{0.8}{\tan(\phi)} \cdot [h(t) - y_i(t)]^{5/2} - [h(t) - z_{top}]^{5/2}] \quad (3)$$

Variables in Equations 1, 2, and 3 are defined visually in Figure 6. The variable i indicates specific sub-openings within the constriction, y_i is the vertical distance between the base of the opening and the upper level of the jam [m], a_i is the height of the orifice [m], ϕ denotes the angle of the weir wing with respect to the horizontal [$^\circ$], and μ denotes the orifice or weir coefficient [-] (standard value of 0.65 coming from clear water hydraulic is considered because the effect of the non-Newtonian nature of a debris flow on it is unknown - Piton and Recking, 2016). The defined geometry of the opening(s) are modified as the simulation progresses to account for jamming.

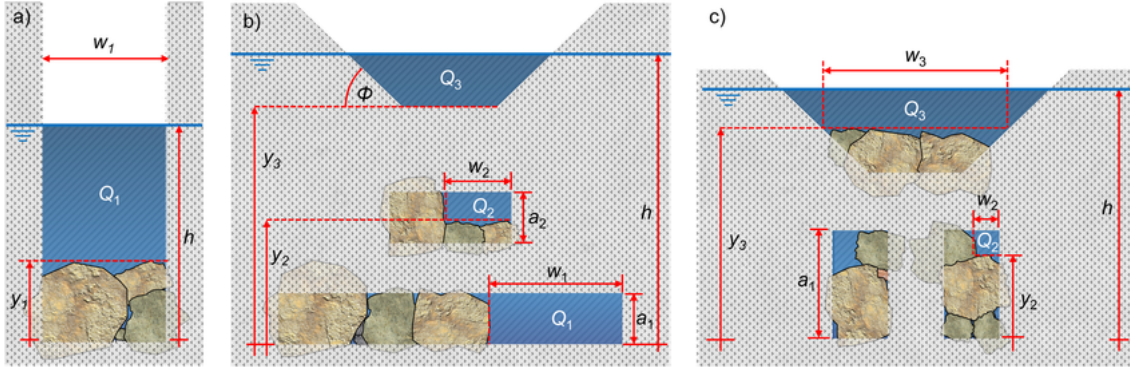


Figure 6: Geometric parameters of possible constrictions. The geometric variables in Equations 1,2, and 3 are visually defined. In a) an example of lateral jamming can be seen. In b), an example of vertical jamming is shown. Figure taken from Piton et al. (2022).

The volume stored in the reservoir ($V(h(t))$) upstream of the constriction is calculated using Equation 4:

$$V(h(t)) = [Q_{in}(t) - Q(h(t))] \cdot \Delta t + V(h(t - \Delta t)) \quad (4)$$

Where $Q_{in}(t)$ is the inflow to the basin [m^3/s], $Q(h(t))$ is the outflow from the basin (through the constriction) [m^3/s], and Δt is the time step duration [s]. Depth $h(t)$, and $V(h(t))$ can be derived from the calculated reservoir volume.

Boulder jamming can occur either laterally or vertically (Figure 1). Lateral jamming occurs when the diameter of the boulder(s) passing through a constriction is greater than the constriction's width. Similarly, vertical jamming occurs when the height of an opening is less than the diameter of the boulder(s) passing through. Lateral and vertical jamming reduces the geometry of the constriction, constraining flow.

Jamming can occur if either the diameter of a single boulder exceeds the size of a constriction, or if two or more boulders reach a constriction at the same time, and their cumulative diameter exceeds the size of the constriction. Thus, jamming is dependent on the spatiotemporal distribution of boulders, and on boulder size. In the Piton et al. (2022) model, these factors are stochastically modeled using a binomial distribution, wherein the size and proximity to the constriction of boulders are randomized for each time step t . The shape of the binomial distribution is defined by the boulder counting estimates, as will be discussed further later.

To stochastically generate boulder size and location within a debris flow event, the Piton et al. (2022) model divides the grain size distribution (estimated through field survey, or literature values) into grain size classes. A binomial distribution is then applied to each grain class (j), randomly generating the number of class- j boulders that pass through the constriction. This procedure is repeated for each distinct grain class, at each time step (t).

For each grain class, the debris flow volume passing through the constriction at time t , hereafter referred to as the "control volume", is divided into "packets", each of which has the same volume as an average class- j boulder. The number of packets is limited by the maximum number of class- j boulders that can exist within the debris flow volume. Equation 5 is used to calculate the number of packets for a given volume.

$$N_j = \frac{V_{control}}{V_j} = \frac{6 \cdot V_{control}}{\pi \cdot D_j^3} \quad (5)$$

Where N_j is the maximum number of packets for boulders of class- j , that are contained within the control volume ($V_{control}$). N_j is also the number of trials required for each boulder class. V_j denotes the average boulder volume within a given class, and D_j is the average diameter.

In reality, the probability of jamming is also dependent on the shape of the boulders. The more spherical particles are, the less likely they are to jam (Zuriguél et al., 2005). Although the model framework assumes that all particles are spherical, all boulders are assessed as class distributions with an estimated upper and lower diameter, defined by the user. When, for instance, the presence of a boulder of diameter class 1 – 2 m is computed, its actual diameter is randomly sampled from the uniform distribution within this range and then compared to the opening size. By assessing jamming in this way, the model indirectly accounts for the variations in sphericity and angularity that would be present in real-world boulders.

The number of boulders in the control volume $V_{control}$ is randomly sampled using a binomial law. The probability (p_j) that a given packet contains a class- j boulder is calculated within a binomial law using its unique calibration parameter. For the most upstream structure, an average number of boulders is accounted for:

$$p_j = \frac{\langle n_j \rangle \cdot V_j}{V_{ref}} \quad (6)$$

Where $\langle n_j \rangle$ is the mean number of boulders of class j within a reference volume V_{ref} (e.g. a former deposit or a dredged volume).

The binomial distribution associated with grain class j is applied to each packet. If the randomly generated number from the binomial distribution corresponds to a "failure" (i.e. a packet not containing a boulder of class j), then the stochastic assessment of the packet is repeated for the next grain class. If the binomial distribution does not "succeed" for a given packet for any of the grain classes large enough to obstruct the constriction, then the packet is assumed to be filled with mud and (and therefore does not cause jamming). This is repeated for all boulder classes, starting at the largest class and working towards the smallest, until the composition of the control volume is fully defined. The size of adjacent packets in comparison to the size of the constriction dictates whether jamming occurs.

There is a great degree of uncertainty associated with debris flow simulation, including parameters such as:

- Total event volume.
- Peak discharge.
- Hydrograph shape.
- Deposition slope.
- The initial capacity of a basin (i.e. the degree of filling prior to an event).
- Degree of clogging due to woody debris and boulders prior to the event.
- The average number of boulders in each grain class.

In the Piton et al. (2022) model, these uncertainties are addressed using possibilistic distributions, wherein the bounds of possibility are defined by an expert (e.g. "in a debris flow event, there will probably be between 1 and 2 Class-1 sized boulders, and there certainly be no less than 0 and no more than 5."). Contrary to a probabilistic analysis (using, for instance, a Monte Carlo approach), a possibilistic approach allows for such crude information without stating a *prior* probability density

function. The possibilistic distributions used by Piton et al. (2022) are defined for a given variable by maximum and minimum values, and either a best estimate, a range of best estimates, or no best estimate. Mathematically, the probability of the variable existing outside of the defined range of maximum and minimum values is zero, and the best estimate is the mode of the distribution (i.e. the most probable value). The possibilistic distributions of all variables are combined to determine the complete range of possible outcomes. The possibilistic analysis was implemented using the HYRISK package (Rohmer et al., 2018).

To speed up simulation times in possibilistic uncertainty propagation analysis, it is possible to state the monotony of the relationship between an input parameter and the output variable, e.g. that the released debris flow volume increases with peak discharge at the inlet (positive monotony) or decreases when the number of boulders increases (negative monotony). To define the monotony of these relationships, a parametric analysis was performed in addition to the real event analysis of the 2005 event (Section 2.3).

2.2.2 Extension of Piton et al. (2022) Framework to a Series of Constrictions

Several updates were made to the Piton et al. (2022) framework to model jamming through a cascading series of constrictions, and under bridges.

Series of structures To model jamming through a cascading series of constrictions, the code is now able to:

- Route the event hydrograph between consecutive structures.
- Route the boulders randomly generated at the first structure directly to the next structures if an "instantaneous" transfer is assumed, or recompute the order and quantity of boulders between consecutive structures, if a "mixing" transfer is specified.

These updates will be expanded upon within this section.

The hydrograph of an event is altered when it passes through a constriction. The framework accounts for this by routing the event hydrograph between structures. The outflow hydrograph from one structure becomes the inflow hydrograph for the structure immediately downstream.

If the channel is uniform in geometry and gradient, lined, and sufficiently narrow to confine and convey all the flows, the order and number of boulders within the surge are unlikely to change over short distances (Figure 7 a-b). Within the model framework, this is referred to as "instantaneous transfer". Debris flows are dynamic processes, however. As the surge flows downstream deposition or erosion may occur through mass exchange with the banks or channel bed, potentially changing the number and order of boulders (Schöffl et al., 2023; Simoni et al., 2020) (Figure 7 c-d). This phenomenon is hereafter referred to as "mixing". Mixing is more likely to occur in a wide, natural, non-uniform channel. For example, a flatter, wider section of the channel or the basin of an open check dam may result in temporary deposition of boulders, which may be later re-entrained. As well, if there are boulders present within the channel from previous debris flow events, or if channel armoring has become loose, they may be entrained within the surge as it flows past.

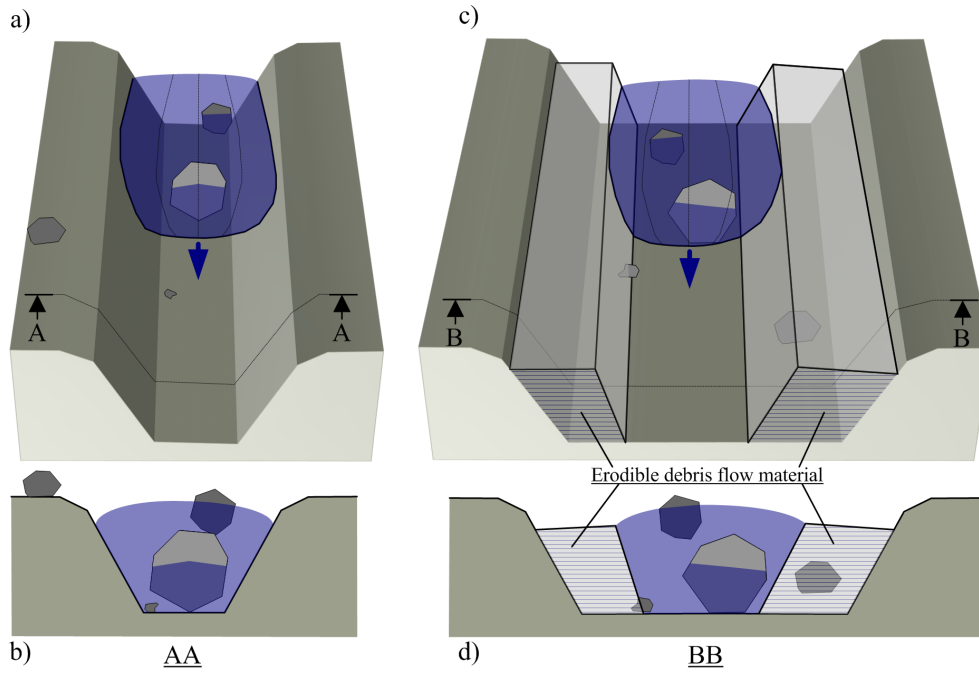


Figure 7: Conceptual visualization of instantaneous transfer (panels a) and b)) where the channel confines the flow and bank and bed are non-erodible, in comparison to mixing transfer (panels c) and d)) of a debris flow between subsequent constrictions.

In the updated model framework, the user specifies whether "mixing" or "instantaneous" transfer occurs between subsequent structures, based on their assessment of the channel. If mixing transfer is selected, the order and number of boulders are re-sampled between constrictions, based on the user-defined "mixing volume" (i.e. the volume of the debris flow within which the order and number of boulders is changed). This re-sampling is performed similarly to the initial boulder sampling performed before the first structure (Section 2.2), however, rather than using the user-defined average number of boulders, the code computes the number of boulders that passed through the upstream structure within the volume of mixing. The resampling methodology is shown in Figure 8. At time step t , the code first finds the duration Δt_{mix} it took for the structure n to discharge the volume V_{mix} through the integral of the outlet discharge:

$$\int_{t-\Delta t_{mix}}^t Q_{out,n}(t) \cdot dt = V_{mix} \quad (7)$$

Once this duration is known, the number of boulders $n_j(t, V_{mix})$ passing the same structure n is counted:

$$n_j(t, V_{mix}) = \sum_{t-\Delta t_{mix}}^t n_{j,n} \quad (8)$$

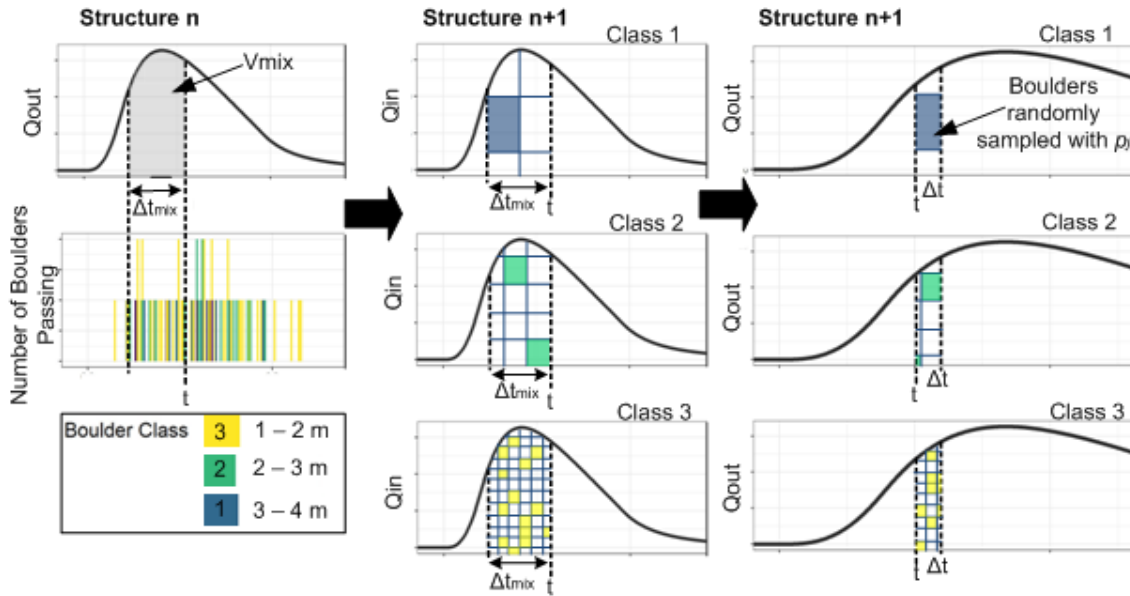


Figure 8: Flow chart explaining how mixing transfer is simulated using the user-defined mixing volume. The panels on the left show the duration (Δt_{mix}) it takes to discharge V_{mix} . The central panel illustrates counting the boulders (n_j) within the same duration. The right panels show how this count is used to compute the boulder presence probability p_j for the random generation of boulders at time t . Note that the computational time step is normally much shorter than the mixing duration ($\Delta t \ll \Delta t_{mix}$.)

As can be seen in Figure 8, at each time step, boulders are re-sampled within the mixing volume for downstream structures, based on the probability (p_j) calculated using Equation 9, where n_j is the number of boulders that pass through the upstream structure (n) within the mixing volume.

$$p_j = \frac{n_j(t, V_{mix}) \cdot V_j}{V_{mix}} \quad (9)$$

If instantaneous transfer is selected, the order and number of boulders are not changed between structures, and the boulders within the surge are not re-sampled.

The type of transfer (instantaneous or mixing) is defined individually for each structure included in the model. In all cases, the model conservatively assumes that the total event volume between structures is conserved, and the only net deposition is that which is explicitly computed as a result of jamming. As part of the parametric analysis, this study examines each transfer type's effect on the jamming analysis results (Section 3.3).

Adding bridges structures The framework was also altered so as to be able to simulate jamming under bridges in addition to debris basins. While the topic of jamming in debris basins during debris flows has been widely studied and published upon, jamming under bridges during debris flows has not. Indeed, to the best of our knowledge, there are no papers published specifically on this topic. Scientific literature on the interaction of debris flows with bridges seems to be largely focused on impact forces rather than jamming, or even hydrodynamics. (Friedl et al., 2024; Wang et al., 2018). Several papers have been published on the topic of woody debris jamming in bridges during clear-water floods (Fenske et al., 1995; Oudenbroek et al., 2018; Jempson, 2000), but debris-flow hydrodynamics are quite different, given their non-Newtonian flow properties. Due to the lack of literature on the topic of jamming under bridges during debris flow events, the updated framework assumes that the

conditions under which the boulders will jam a vertically confined debris basin are equivalent to those that will jam a bridge. These conditions are conceptually shown in Figure 9.

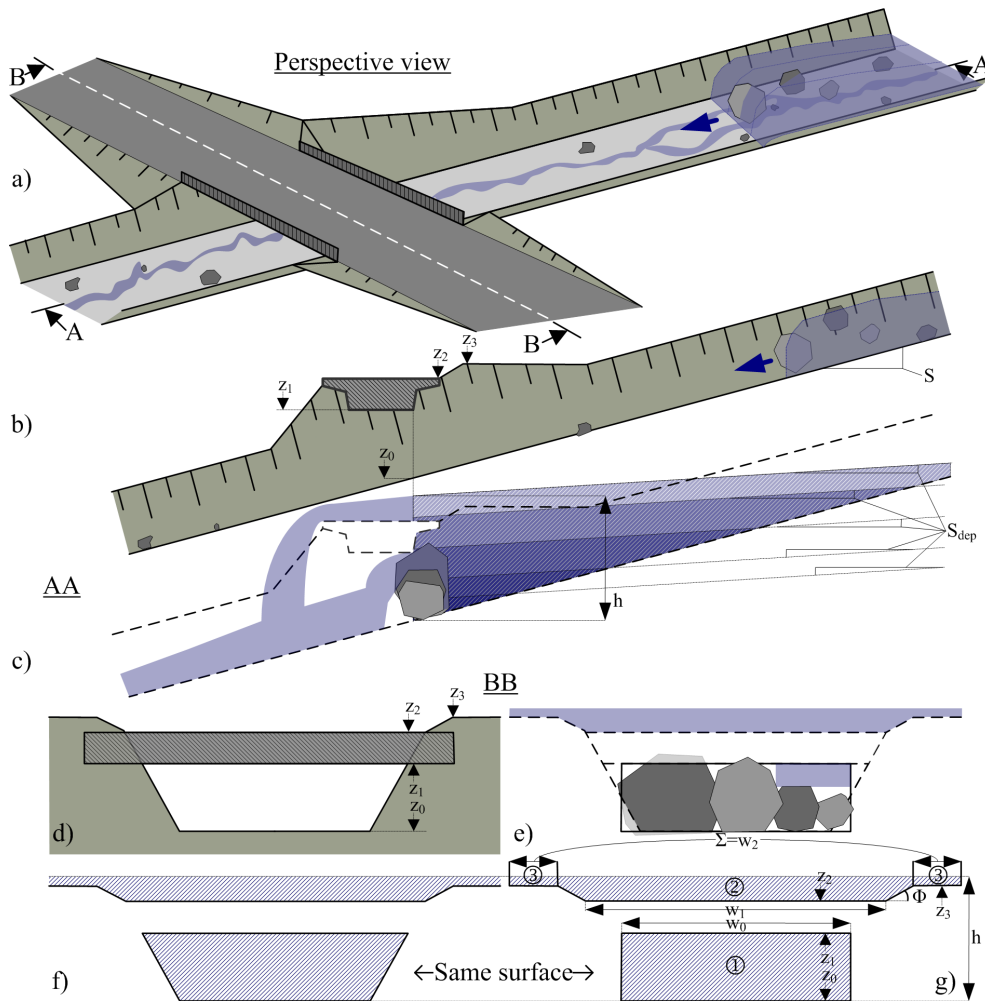


Figure 9: Conceptual demonstration of jamming under a bridge a) Schematic perspective view of a bridge and a debris flow; b) Longitudinal profile of the structure; c) Schematic longitudinal profile representing the constant-slope filling of the channel upstream of the bridge for a variable flow height h ; d) Cross-sectional profile of the structure; e) Schematic cross-sectional profile representing a partially obstructed structure. The blue sections represent the flow cross-sections for the obstructed state shown; f) Schematic cross-section representing the actual maximum flow cross-section; g) Schematic cross-section representing the maximum flow cross-section as modeled (composition of vertical-walled weirs, trapezoidal weirs and rectangular orifices with cross-sections, widths and heights close to the actual cross-sections in order to present an equivalent flow rate and similar propensity to blockage by boulders).

In general, a debris basin and a bridge are quite similar, in that they are both structures that cause a constriction within the channel. The main geometric difference between the two is that under bridges, the channel often retains its width and gradient, as the goal of the structure is conveyance rather than attenuation. Conversely, debris basins are often preceded by a sediment trap - a wider, flatter section of channel that encourages deposition (Piton et al., 2024).

Although in practice, debris basins are often preceded by a sediment trap, many laboratory experiments have studied jamming in open check dams without an upstream sediment trap, and with a

consistent channel slope (e.g. Sun et al., 2018; Goodwin and Choi, 2020; Dong and Pu, 2024; Yuan et al., 2019), thus with a configuration similar to a bridge. In the Yuan et al., 2019 study, jamming of a grid-type dam during a debris flow event was experimentally studied using a flume with a consistent slope. This study found that if the ratio of the size of the dam openings to the maximum particle size ($Opening\ Size/D_{max}$) is 0.5-1, full blockage occurs, and if the ratio is 1.5-2, partial blockage occurs. Although there was no sediment trap upstream of the grid-type dam in this experiment, these results tend to agree with the generally accepted guidelines for when jamming is expected in debris basins with an upstream sediment trap ($Opening\ Size/d_{max} = 1.5$, Piton and Recking, 2016). Similar experimental configurations (i.e. a check dam without an upstream sediment trap) were used in other studies (Sun et al., 2018; Goodwin and Choi, 2020; Dong and Pu, 2024) and similar results were found.

Based on the similarity of the conditions under which jamming of open check dams has been found to occur in experiments with and without upstream sediment traps, in the updated framework, jamming through bridges is simulated using the same blocking criteria as for barriers. Unlike open check dams with an upstream sediment traps, the volume – elevation curve for the area immediately upstream of a bridge does not need to be inputted into the model. Instead, it is automatically generated based on the inputted channel slope and width. Although in reality, the areas beneath a bridge can be many shapes, for simplicity the updated framework approximates the cross-section as rectangles separated by piles, and in the simplest case of pile-less bridges, as one rectangle (Figure 9). The bridge’s storage capacity $V(h, S_{dep})$ is computed as:

$$V(h, S_{dep}) = \frac{w_0 \cdot h^2}{2(S - S_{dep})} \quad (10)$$

Where w_0 is the rectangular equivalent mean width of the upstream channel (m), S is the channel slope (m/m) and S_{dep} is the deposition slope (m/m).

As culverts have similar structural geometry and purpose to bridges, they can also likely be modeled using the updated framework. As there are no culverts in the alluvial fan of the Torrent du Saint-Martin however, modeling culverts is outside of the scope of this work, and this assumption remains untested.

In addition to the extension of the framework to allow modeling of debris flows through a series of structures, and through bridges, several general adjustments were made to the existing code. These adjustments are detailed in Appendix B.

The modeling framework, including all of the updates outlined in this section, is freely available through an online interface at <https://platrisk.ige.inrae.fr>. The code is open source and available on GitHub where it can be downloaded for R.

2.2.3 Plain Language Summary of Framework

The framework possibilistically models jamming caused by large boulders as debris flows pass through constrictions. Possibilistic analysis is an alternative statistical framework to a probabilistic analysis, wherein practitioners are able to calculate the full range of possible outcomes based on limited input data (bounds and eventual best estimates). The required input variables are:

- Event volume,
- Peak flow,
- Time to peak,

- Deposition slope,
- Quantity and grain size distribution of boulders within the event,
- Geometry of constriction(s)
- Initial jamming or deposition upstream of constriction(s).

Prior to running the simulation, the user is required to possibilistically bracket the input variables with a maximum value, a minimum value, and if possible either a best estimate, a range of best estimates. For example, a practitioner may decide that there will most likely be 5, 4-5 m boulders within a debris flow event, but there will definitely be no more than 10, and no less than zero.

For each time step within the model:

1. The volume and depth of debris flow upstream of the constriction is calculated using basic hydraulic equations and conservation of mass principles.
 - (a) Flow through the constriction is calculated using either the weir equation, the grand orifice equation, or the slit equation. Equations are selected based on the inputted geometry of the opening(s).
 - (b) The volume of debris flow both upstream and downstream of the constriction is calculated using basic conservation of mass principles and the volume-elevation curve of the basin.
2. Boulders are stochastically generated within the volume of debris flow currently passing through the constriction.
 - (a) The volume of debris flow currently passing through the constriction is divided into "packets". Each packet has the same volume as an average boulder in a given grain class.
 - (b) Boulders are stochastically generated within the packets using the user-defined binomial probability associated with the given grain class.
 - (c) If the stochastic assessment "fails" for a given packet, then the stochastic assessment is repeated for the next grain class. If the stochastic assessment "fails" for all grain classes, then the packet is assumed to be composed of fluid, and therefore will not cause jamming. This is repeated for all packets for all grain classes, starting at the largest grain class and working towards the smallest until the composition of the debris flow passing through the constriction is completely defined.
3. Jamming is simulated. If the diameter of a boulder exceeds the height of the constriction, or if two or more boulders with a combined diameter exceeding the width of the constriction reach the constriction at the same time, jamming occurs.
4. If jamming occurs, then deposition is assumed to occur behind the jam, filling the basin/ channel at the deposition slope defined within the input variables. As well, the geometry of the constriction is updated for subsequent time steps to account for the jam that decrease the opening section.
5. This process is repeated until the entire hydrograph is complete at the most upstream structure.
6. The outflow hydrograph from the upstream structure becomes the inflow hydrograph to the structure immediately downstream.
7. The entire process is repeated, until jamming has been simulated at all structures, starting at the upstream structure, and working towards the downstream. If the user specifies a "mixing" transfer, boulders are re-generated between structures.

2.3 Case Study Procedure

Two simulations were conducted using the updated modeling framework (Section 2.2): a re-creation of the June 2005 event (Section 2.1.3), and a parametric analysis. The June 2005 event was modeled to compare the results of the updated framework against a known historical event. It explores the validity of the approach. The purpose of the parametric analysis was to assess the sensitivity and the monotony of the input variables. The positive/negative correlations between the input variables and the model results were used to define the monotony within the code, to increase the model's computational speed. The input parameters used to simulate jamming within the Torrent du Saint-Martin are summarized in Section 3. They were measured, researched, or estimated using a variety of methods, which are expanded upon here.

2.3.1 2005 Event

The June 2005 event was simulated both as a "normal run" assuming known input parameters (i.e. only the best estimate values are used for calculations), and then with a full uncertainty propagation analysis. The "normal run" was included in the study as a proof of concept, to demonstrate the updated framework's capabilities in a simple, easy-to-follow format. The possibilistic analysis was conducted with 25 runs (enough to provide statistically significant, replicable results). Minimum, maximum, and best estimate values were required for all input parameters (Piton et al., 2022). The integration of these ranges of variables into the modeling framework is explained further in Section 2.2. All parameters used to simulate the 2005 event are summarized in Appendix C.

Structure Geometry The geometry of the structures included in this study (the Upper Debris Basin, Lower Debris Basin, and Upper Bridge) is summarized in Figure 10. All measurements were approximated based on a field visit and the Lidar of the Torrent du Saint-Martin's alluvial fan collected by the RTM in 2017.

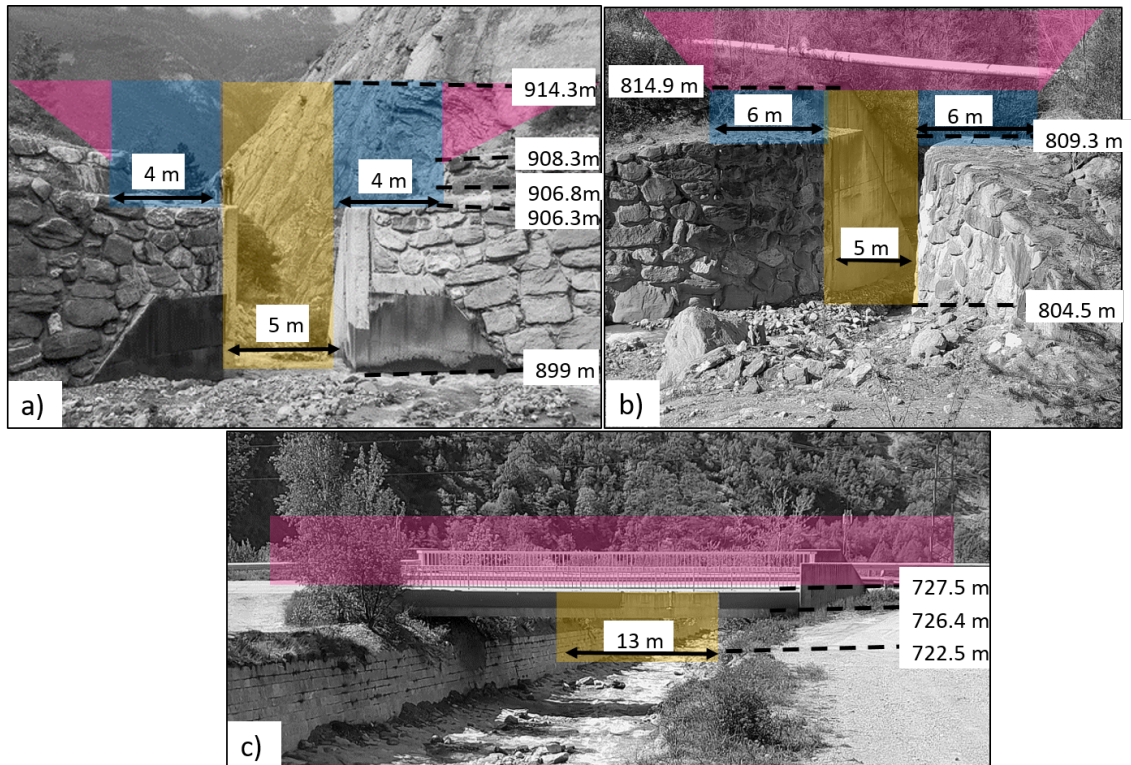


Figure 10: Geometry of the a) Upper Debris Basin, b) Lower Debris Basin, and c) Upper Bridge as approximated from the 2017 Lidar, and field measurements. The colored shapes depict how the geometry is divided for modeling. Panel a) courtesy of G. Piton, Panels b) and c) from Carladous et al., 2022.

Volume-Elevation Curves Volume-elevation (VE) curves of the Upper and Lower Debris Basins were developed in Global Mapper using the 2017 Lidar, which was also used to measure the channel width and slope upstream of the bridge. The methodology for VE curve development is presented in Appendix D.

Deposition Slopes The range of deposition slopes was estimated based on deposition slopes recorded from historical debris flow events along the Torrent du Saint-Martin and engineering design assumptions (Piton et al., 2020; ONF-RTM, 2013). These slopes are shown in Figure 11, and were in general agreement with the slope of the alluvial fan (the natural angle at which deposition of debris flow events has historically occurred over many events), measured from the 2017 Lidar. The median value of recorded deposition slopes was selected as the best estimate deposition slope. The minimum and maximum values were selected as the minimum and maximum bounds for modeling (Figure 11).

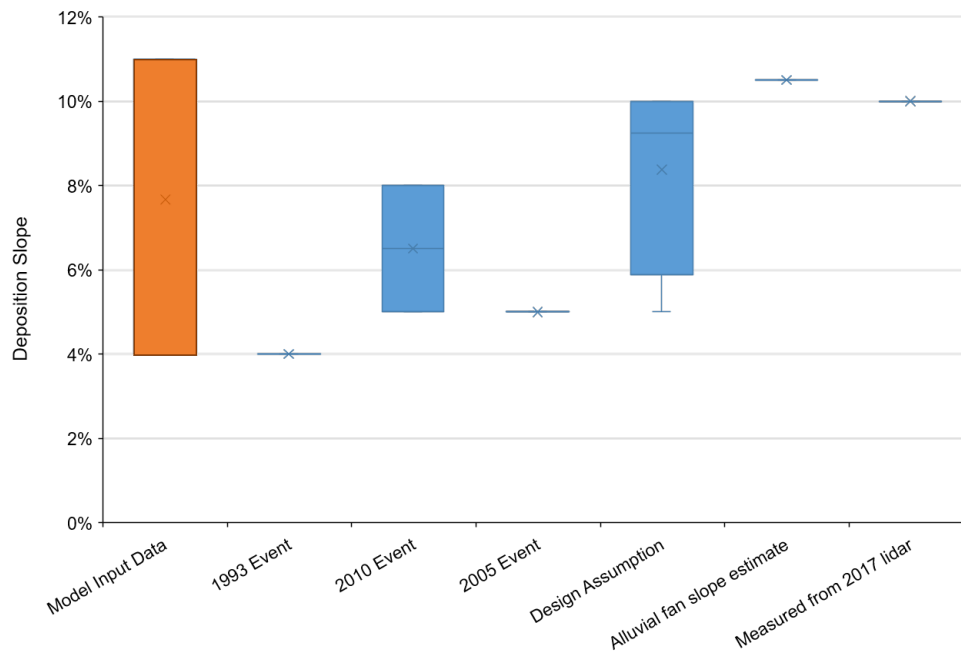


Figure 11: Distribution of literature values for disposition slope, measured from historical events (ONF-RTM, 2013), or estimated by professionals for design purposes (ONF-RTM, 2013; Piton et al., 2020). The minimum, maximum, and best estimate deposition slopes adopted for modeling were based on these values.

Event Volume The 2005 event was categorized as "exceptional", with a return period of greater than 100 years (ONF-RTM, 2013). The best estimate volume was assumed to be that of an exceptional event reported in (ONF-RTM, 2013). The minimum and maximum values were set to the minimum and maximum values estimated for each event using the variety of methods presented in Table 1.

Peak Flow While ONF-RTM (2013) provides a range of peak flows associated with the various event categories, it does not provide a best estimate. The peak flow associated with the best estimate event volume was therefore calculated using various empirical equations (Mizuyama et al., 1992; Bovis and Jakob, 1999; Rickenmann, 1999; Ikeda et al., 2019; Mitchell et al., 2022). Assuming a triangular hydrograph, the Mizuyama et al. (1992) equation for muddy debris flows fit best with the range of peak flows and the event durations reported in ONF-RTM (2013). As such, the values calculated with this empirical relationship were used as the peak flow best estimate. The upper and lower bounds reported in ONF-RTM (2013) were used as the upper and lower bounds for modeling.

Time to Peak The time to peak was estimated based on the triangular hydrograph methodology presented in Marchi et al. (2021), where simplified triangular hydrographs were developed from events recorded in the Italian Alps between 1990 and 2019. In this study, three simplified hydrographs are presented, ranging from low to high event severity. The Marchi et al. (2021) study was based on data gathered in the Italian Alps - relatively close to the Torrent du Saint-Martin. As well, we corroborated the methodology with several other debris flow studies conducted in similar geographic locations: Ilgraben, Switzerland (Raffaele Spielmann, 2022; Swartz et al., 2004), Randa, Austria (Arai et al., 2014; Schimmel et al., 2022), Moscardo, Italy (Arattano and Marchi, 2008; Arattano et al., 2012), Gadoria, Italy (Coviello et al., 2021; Nagl et al., 2020; Coviello, 2015; Arattano et al., 2016), the Italian Dolomites (Berti et al., 2000), and the French Alps (Lapillonne et al., 2023; Navratil et al.,

2012). In these studies, the times to peak measured from the event hydrographs were all within the range presented by Marchi et al. (2021) (Figure 12). As well, the Marchi et al. (2021) methodology has been applied to hydrograph creation in other debris flow studies (Mitchell et al., 2022).

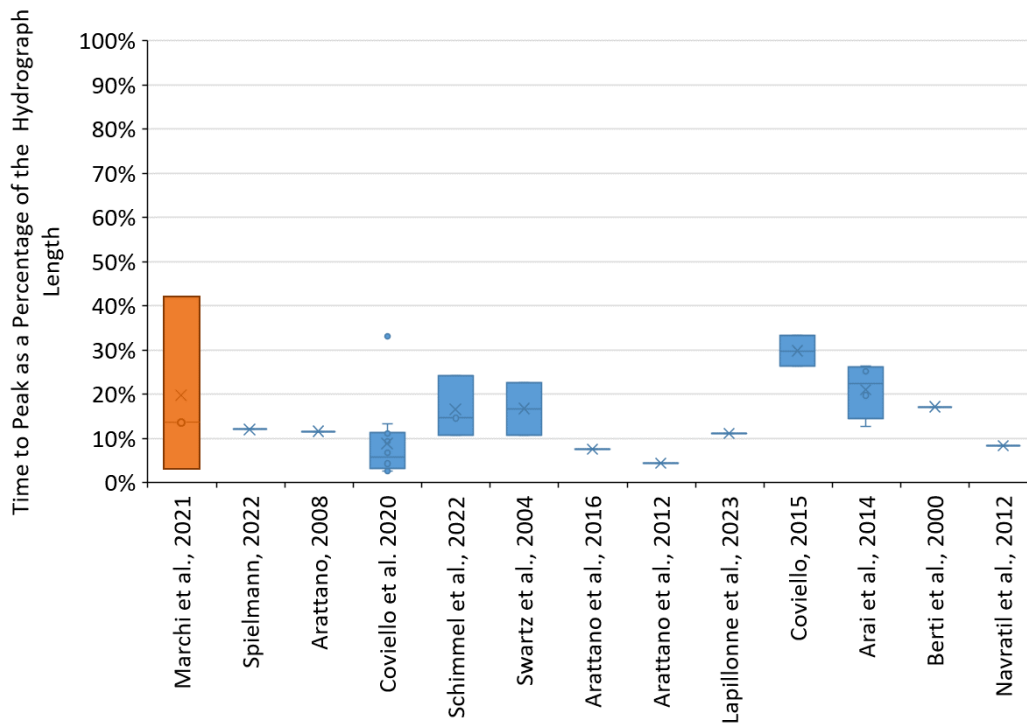


Figure 12: Distribution of time to peak from various debris flow hydrographs measured close to the Torrent du Saint-Martin. All of the measured time to peaks fall within the range proposed in Marchi et al., 2021, validating the application of this methodology to create a maximum, minimum, and best estimate of time to peak.

Initial Conditions The mitigations within the alluvial fan of the Torrent du Saint-Martin are well-maintained, and the debris basins are generally cleared after large events (ONF-RTM, 2013). We therefore assumed that there was no initial jamming and no initial deposition upstream of the three constrictions prior to the 2005 event.

Boulder Class Distribution The boulder classes and the number of boulders present within a debris flow event were estimated based on a May 2024 site visit, and historical debris flow records found in the archives of the RTM (n.d.). During the site visit, boulders deposited within the channel were measured and counted to estimate boulder size from historical debris flow events. The observed boulders were divided into classes, and the representative volume ($10,500 m^3$) was estimated by multiplying the channel width by the length of the channel within which data was collected, and assuming that a 1 m thick layer of boulders was visible. Assuming all boulders were spherical, it was estimated that they composed 14% of the representative volume. Boulders smaller than 0.5 m were not counted, as they are too small to jam in any of the structures included in this analysis (width > 6 m and height > 4 m). Similarly, although boulders with diameters ranging from 0.5-1 m were counted during the site visit, these were also eventually discarded from the analysis, as they too are likely too small to cause jamming within the structures included in this analysis. Discounting the 0.5-1 m diameter

boulders, it was estimated that boulders composed approximately 10% of the representative volume. The boulder classes found during the site visit are summarized in Table 2.

Table 2: Summary of the boulder class distribution found in the channel during the 2024 site visit. 0.5-1 m boulders were not included in the analysis, as they were deemed too small to jam any of the structures included in this study (width > 6 m, height > 4 m)

Boulder Class	Number of Boulders	Percentage of Representative Volume
0.5 -1 m	2123	N/A
1 -2 m	320	5%
2 -3 m	28	2%
3 -4 m	6	1%
4 -5 m	2	1%

The volume of boulders and the total volume of material cleared from debris basins along the Torrent du Saint-Martin following debris flow events in 2005, 2008, and 2010 are available in the RTM’s archives. In one source, it was stated that any rock with a volume greater than 0.4 m^3 (i.e. a diameter of 0.9 m, assuming a spherical shape) was considered a boulder for record-keeping purposes. We assumed that this classification was consistently applied throughout all records. Using this data, the proportion of boulders as a percentage of deposited volume could be calculated. Results ranged from 0.4% to 2.2%. The 2005 event had a 1.1% proportion of boulders (RTM, n.d.).

There is variability in the proportion of debris flow volume composed of boulders found in the historical records of debris basin dredging (0.4 - 2.2%), and when counting the proportion of boulders found in the bed during the 2024 site visit (10%). When debris flows naturally deposit on an alluvial fan, over time, smaller sediment particles are transported downstream. Boulders, however, are less easily re-mobilized, and may only be transported by erosive debris flow events. Therefore, over time the grain size distribution of material within the channel skews larger - a phenomenon referred to as channel armoring. This phenomenon likely impacted the results of the site visit but would have had a smaller impact on the proportion of boulders found in the historical records, as the decreased slope of the debris basins is designed to facilitate deposition (and would therefore be more likely to retain small sediment particles). As well, the debris basins were cleared soon after debris flow events, so the data would not be impacted by years of size-selective sediment transport.

For modeling, the percentage of the event volume composed of boulders was informed by both the 2024 site visit and the historical data from the RTM archives (RTM, n.d.). The lower bound was set to equal the lowest percentage of boulders found within the historical records (RTM, n.d.). The best estimate was set equal to the proportion of boulders found within the representative volume cleared from a debris basin following the June 2005 event (RTM, n.d.).

The upper bound is more exploratory. It was calculated by assuming a complete bed mobilization along the alluvial fan during the exceptional event (Table 1) (the event that was selected to simulate the 2005 event (Section 2.3.1). Based on estimated erosion rates, full bed mobilization along the alluvial fan could contribute approximately $40\,000 \text{ m}^3$ of material to the debris flow (ONF-RTM, 2013). It was assumed that this $40\,000 \text{ m}^3$ would have a 10% boulder concentration (per the 2024 site visit (Table 2). The rest of the event volume for the exceptional event was assumed to have the same proportion of boulders as the material cleared from a debris basin following the 2005 event (RTM, n.d.).

The distribution of boulders found during the 2024 site visit was also exploratory. First, the distribution of boulders found during the 2024 site visits was used to estimate the ratio of 1-2m boulders in comparison to the 2-3m boulders (11:1). The number of 3-4 m and 4-5 m boulders within

the 2005 event was then estimated using another approach based on a combination of engineering judgment, and anecdotal records of historical debris flow events within the Torrent du Saint-Martin. Very few boulders of such great size were found in the channel (Table 2); neither were many found within debris flow deposits according to historical records. Such boulders are also difficult to mobilize and convey. Since there is no record of the Lower Debris Basin stopping such large boulders, or of them depositing further downstream during the 2005 event, we hypothesize that all of them were trapped by the Upper Debris Basin. The counting of the few boulders of this category and their average presence was consequently not considered at the scale of the basin deposit, or at the scale of the representative volume from the site visit (i.e. 10 000 m^3) but rather at the scale of the full event (i.e. 157 500 m^3).

When this distribution was applied to the Torrent du Saint-Martin however, jamming was simulated in the Lower Debris Basin in even the frequent event (with a return period of approximately 10 years). As we were anecdotally informed by the RTM that the Lower Debris Basin has never experienced jamming (a fact that is corroborated by a lack of recorded Lower Debris Basin jamming in any historical record of the Torrent du Saint-Martin we were able to find), this result is unrealistic. Since most simulated jamming was caused by 2-3 m boulders, the ratio of 2-3 m boulders and 1-2 m boulders was approximately halved, and the simulation repeated, with more realistic results (i.e. no predicted jamming in the Lower Debris Basin during the frequent event).

The distribution of boulders between classes found within the channel during the 2024 site visit may also have been affected by size-selective transport (channel armoring) effects, resulting in a greater ratio of large boulders to small boulders than would typically be observed during a debris flow. We recommend that practitioners be wary of this when gathering field data for future simulations of other sites, especially if an overabundance of historical data is not available for model calibration (as is the case for the Torrent du Saint-Martin).

There is uncertainty associated with the boulder size and number estimation methodology. During the 2024 site visit, it was noted that boulder size tended to increase with elevation, skewing the boulder class distribution towards the larger sizes. This means that the results of the field study would vary with collection location. This is likely partially due to a filtering effect applied by the debris basins, which are wider and flatter than the upstream channel, encouraging deposition. Data was collected from below the Upper Bridge to upstream of the Upper Debris Basin, although portions of the channel were inaccessible due to high flows. As well, The Upper and Lower Debris Basins appeared to have been cleared since the latest debris flow event, so boulders trapped by the debris basins could not be counted. Finally, boulder quantity and size vary between debris flow events based on factors such as event size, triggering mechanism, and debris availability. The RTM's historical records (RTM, n.d.) are only representative of the material found within one basin following an event, and not of the event itself. There is therefore uncertainty surrounding the estimation of the number and size of boulders present in the June 2005 event, but the combination of the observations from the site visit and the historical records were assumed to produce a reasonable approximation.

Mixing Volume The 2005 event reportedly damaged the channel armoring within the alluvial fan (ONF-RTM, 2013), indicating that mixing occurred. In addition, many boulders were observed in the intermediate channel during the 2024 site visits, which a large debris flow event could entrain. Finally, although records indicate that the Lower Debris Basin has historically been cleared of boulders and other debris following debris flow events (RTM, n.d.), the Lower Debris Basin itself would facilitate deposition and re-entrainment of boulders within the debris flow surge as it's width and gradient are designed to facilitate – transient – deposition. Because of these reasons, all transfers between structures were assumed to be "mixing" when simulating the 2005 event.

The mixing volume between structures was assumed to be equal to the surface area of the channel (including the Lower Debris Basin) between constrictions multiplied by an arbitrarily fixed 1 m thick layer of debris, conservatively assuming full-bed mobilization during the event. This hypothesis was equivalent to assuming a potential erosion rate of 7 - 12 m³/m of channel, a relatively high but realistic order of magnitude in debris flow channels near fan apexes (Hung et al., 1984; Theule et al., 2015; Torresani et al., 2023).

For each set of parameters, 25 iterations were completed, which was sufficient to observe consistent and repeatable patterns in the results.

2.3.2 Parametric Analysis

For the purposes of the parametric analysis, the rare event (Table 1) was selected, as it was experimentally found to generally partially block the Upper Debris Basin. The return period of this event is approximately 100 years (Table 1), in comparison to the return period of the 2005 event, which is greater than 100 years.

A "normal run" was conducted for the parametric analysis (i.e. only the best estimate value was used for calculations, rather than the upper and lower bounds which would be used in a full uncertainty propagation analysis). For each set of parameters, 100 iterations were completed, which was sufficient to observe statistical significance (i.e. consistent and repeatable patterns) in the results.

The input variables tested in the parametric analysis are:

- Initial jamming of the structures,
- Peak flow,
- Deposition slope,
- Time to peak,
- Event volume,
- Number of boulders,
- Mixing volume.

All input parameters were carried over from the simulation of the 2005 event (Section 2.3.1). The effect of each input variable on the model was analyzed by modifying the best estimate value to be equal to first the lower limit and then the upper limit. The exceptions to this methodology are the event volume and peak flow (which were instead set to those associated with the rare event), the initial jamming conditions, and the mixing volume (which do not have an upper/ lower limit). These parameters were varied using engineering judgment.

For the analysis of most input parameters, only one structure (the Upper Debris Basin) was modeled. To analyze the monotony of the mixing volume, however, a transfer between structures was necessary, so the Lower Debris Basin was simulated as well. Input parameters used for each sensitivity case are included in Table 6.

3 Results

3.1 Definition of Final Input Parameters

The minimum, maximum, and best estimate event volumes are summarized in Table 3, and the peak flows are summarized in Table 4.

Table 3: Summary of minimum, best estimate, and maximum event volumes selected for modeling.

Event	Parametric Analysis	2005 Event
Minimum Volume (m^3)	24 000	70 000
Best Estimate (m^3)	80 000	150 000
Maximum Volume (m^3)	150 000	250 000

Table 4: Summary of the peak flows associated with the minimum, best estimate, and maximum event volumes.

Event	Parametric Analysis	2005 Event
Minimum Peak Flow (m^3/s)	100	200
Best Estimate (m^3/s)	140	233
Maximum Peak Flow (m^3/s)	250	350

The time to peak from Marchi et al. (2021)'s low, medium, and high severity hydrographs (3%, 14%, and 42% of the event duration) were adopted as the minimum, best estimate, and maximum time to peak for modeling both the parametric analysis, and the 2005 event.

The minimum, maximum and best estimate deposition slopes were 4%, 8% and 11%.

The number of boulders estimated in each class within a representative $157\,500\,m^3$ of debris flow are shown in Table 5.

 Table 5: Boulder class distributions selected for modeling within a representative $157\,500\,m^3$ of debris flow.

Boulder Class	Number of Boulders		
	Lower Limit	Best Estimate	Upper Limit
Proportion of Representative Volume	0.4 %	1.1%	3.4%
1 – 2 m	270	550	1700
2 – 3 m	27	55	170
3 – 4 m	0	11	34
4 – 5 m	0	1	4

With the selected boulder distribution and proportion of boulders, the frequent event (with a return period of approximately 10 years (Table 1) rarely jams the Upper Debris Basin when modeled. Historically, small, routine events have not resulted in jamming of the Upper Debris Basin. The results from the simulation of the Upper Debris Basin during the frequent event are included in Appendix E. Conversely, the rare event (with a return period of approximately 100 years (Table 1) sometimes jams the Upper Debris Basin. Although uncertainty remains regarding the selected boulder distribution, the simulation results are consistent with empirical observation. This validates the selected boulder proportion and distribution, as the Upper Debris Basin has historically only jammed in higher return period events (which reduces maintenance costs) (Carladous et al., 2022). (Section A).

The 2005 event was simulated with a mixing volume of $5600\,m^3$ between the Upper Debris Basin and Lower Debris Basin, and $5000\,m^3$ between the Lower Debris Basin and the Upper Bridge.

For the parametric analysis, the mixing volume was set to $5600\,m^3$, $560\,m^3$, and $56\,m^3$ - the mixing volume used to simulate the 2005 event and a mixing volume one order of magnitude, and two orders of magnitude smaller (which was selected to study the sensitivity of the model results to the inputted mixing volume). The effects of the mixing volume were compared to a simulation where instantaneous transfer was assumed. The parametric analysis for the mixing volume was completed with four data

points (as opposed to three, like the other input parameters) because relatively little is known about mixing within debris flows, making it difficult for practitioners to accurately constrain. The additional data point allows us confidence in our assessment of the monotony.

To simulate the 2005 event, it was assumed that there was no initial jamming or deposition. For the parametric analysis, three initial jamming conditions were analyzed: no jamming, a 1.5 m jam with no deposition, and a 3 m jam with no deposition. These initial conditions were selected based on the size of the boulders observed in the channel during a May 2024 site visit.

3.2 2005 Event

The June 2005 event was simulated both with a "normal" run, and with a full possibilistic uncertainty propagation analysis. Sample output from the normal run of the Upper Debris Basin are shown in Figure 13. All figures produced by the analysis are available in Appendix E.

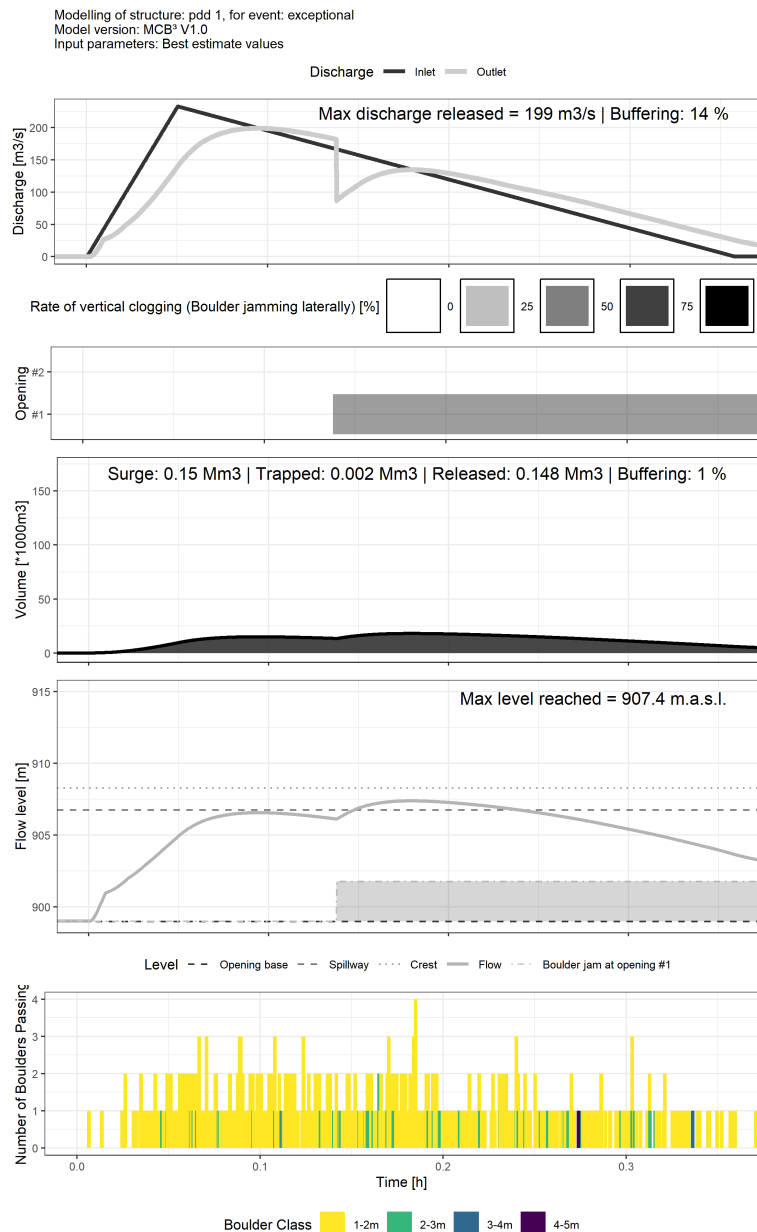


Figure 13: Discharge, clogging, flow level, volume, and generated boulders in the Upper Debris Basin from one "normal" run, simulating the 2005 event.

In Figure 13, it can be seen how the hydrograph is modified by both the flow through the constriction and by clogging. The hydrograph abruptly decreases when jamming occurs, before increasing again. The outflow volume and the flow level are similarly modified by the jamming, with an inflection point in both graphs visible when the jamming occurs. Jamming is dependent on the number and size of generated boulders. Only 1% ($\approx 2000 m^3$) of the debris flow volume was buffered by the Upper Debris Basin in this simulation.

The possibilistic simulation results showing the Upper Debris Basin are displayed in Figure 14 as a sample of the model's capabilities. Similar results for the Lower Debris Basin and the Upper Bridge are included in Appendix E.

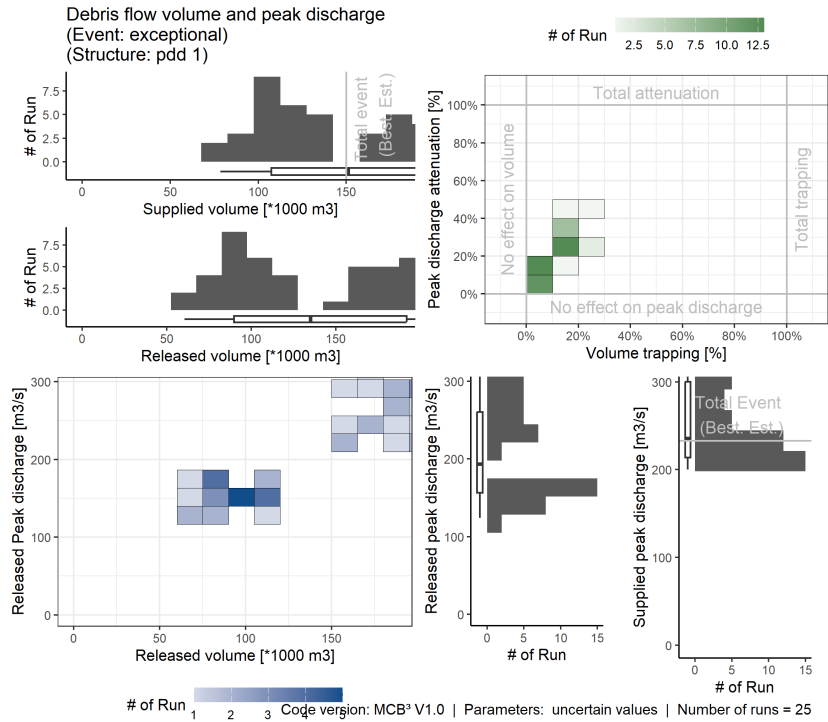


Figure 14: Results of the possibilistic analysis of the Upper Debris Basin, from the simulation of the June 2005 debris flow event.

In Figure 14, it can be seen that the Upper Debris Basin had a small, but non-negligible effect on the released volume and the released peak discharge, through debris flow attenuation. The released peak flow and released volume is less than the supplied volume and peak flow. The released volume varied between approximately 50 000-200 000 m^3 . The released peak discharge varied between approximately 100-300 m^3/s , increasing with the released volume.

The results of the possibilistic analysis in comparison to historical records of the 2005 event (ONF-RTM, 2013) are shown in Figure 15.

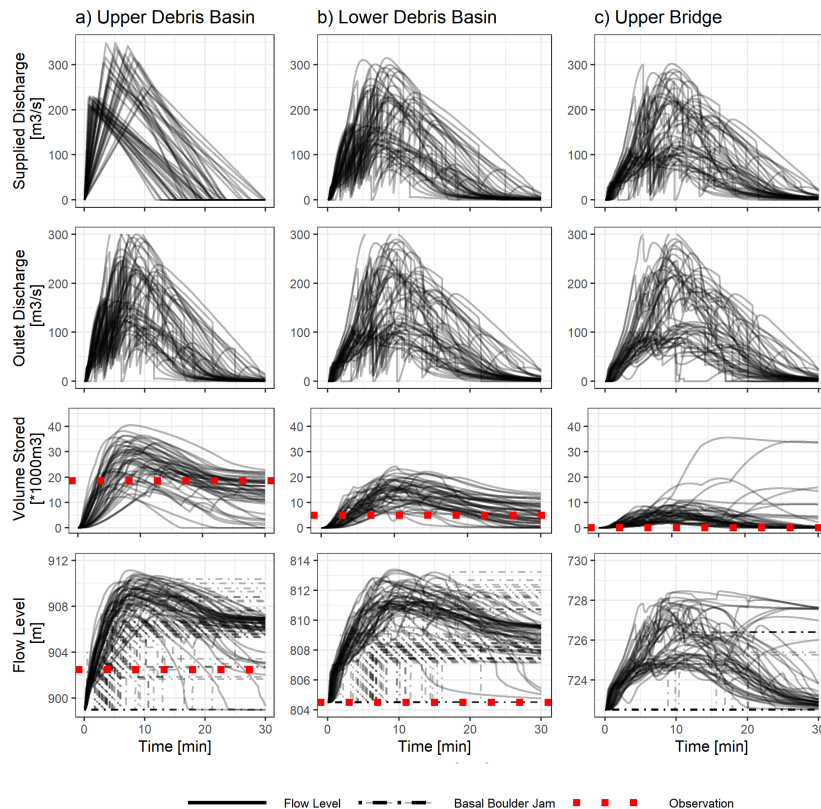


Figure 15: Results of the possibilistic analysis of the Upper Debris Basin, Lower Debris Basin, and Upper Bridge, showing each simulation in comparison to historical records of the June 2005 debris flow event (ONF-RTM, 2013), shown in red.

When simulating the 2005 event, approximately 1 in approximately every 50 simulations was unable to converge on a solution. This can likely be attributed to the steepness of the channel slope at the Upper Bridge (10%), which is close to the upper bound of the inputted deposition slopes (11% (Section 3.1)). If the Upper Bridge clogs and there is a steep deposition slope, the length of the deposition approaches infinity, thus making the mass balance equation (Equation 4) unable to converge. Should this issue occur in future simulations of other sites, we recommend that either only the completed runs are used for the analysis, or that the analysis is repeated until the random selection of boulders and depositions slopes aligns in such a way that convergence is achieved for all simulation runs.

3.3 Parametric Analysis

The results of the parametric analysis are shown in Figure 16

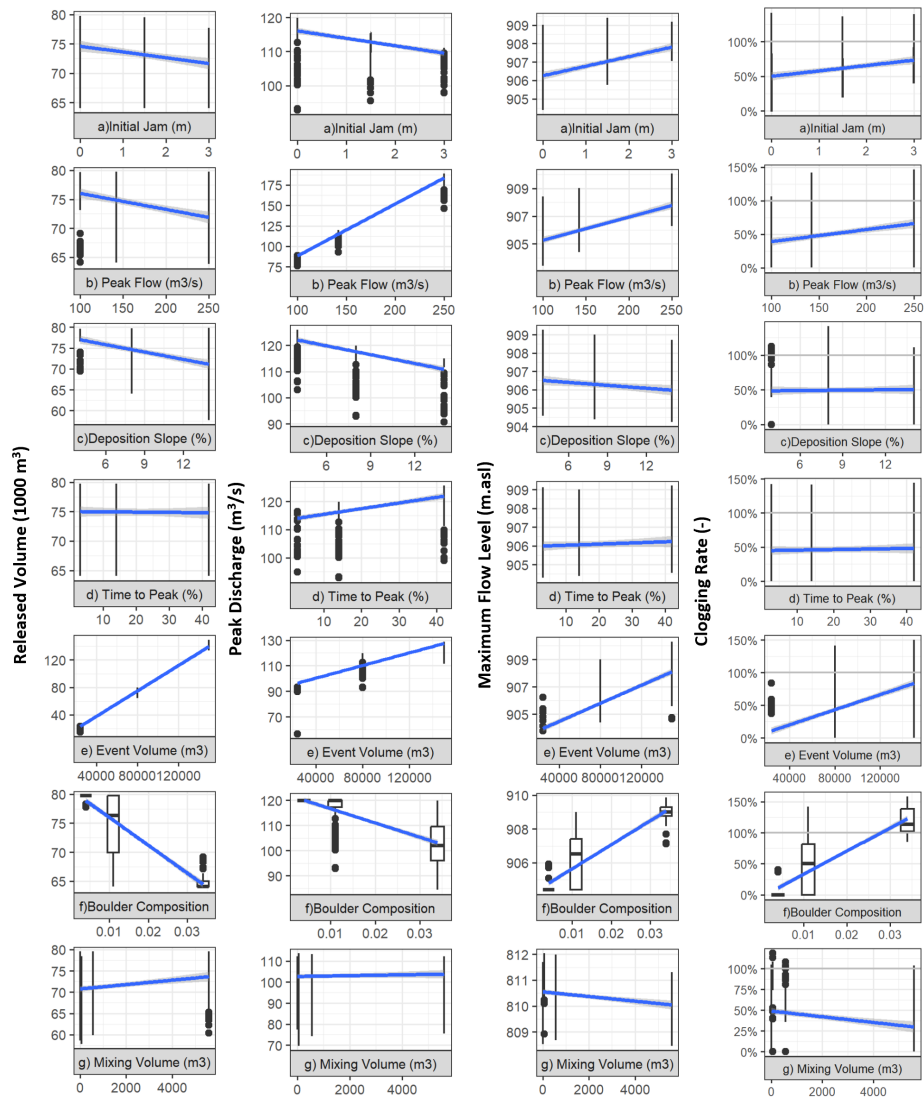


Figure 16: Parametric analysis results, showing the monotony of outflow volume, peak outflow, maximum flow level, and clogging rate with the variation of input variables. Note that for ease of graphical representation, the instantaneous transfer scenario (row g) is shown as having a mixing volume of 0 m^3 . In reality, these two scenarios are not equivalent, as boulders are not regenerated between structures during an instantaneous transfer.

A summary of the parametric analysis results is presented in Table 6. Overall, most model inputs (with the exception of event volume and peak inflow) had a minor impact on the model results, varying the outflow volume and peak outflow by 15% or less. This indicates that concerning the Torrent du Saint-Martin, the model is robust in the face of uncertainty. This conclusion might be site-specific however, and may not apply to other steep creeks. When modeling other sites, it is recommended that the model framework is applied using the uncertainty propagation module, thereby reducing the model’s sensitivity to selected input values by explicitly accounting for uncertainty. The implications of the parametric analysis results are further discussed in Section 4.2.

Table 6: Monotony highlighted by the parametric analysis, i.e. effect on the output parameters of a variation of the input parameters. Results marked with an * are statistically significant ($p < 0.05$).

The best estimate values used in the simulation of the 2005 event are **bolded**

Input parameter	Values Tested	Units	V_{out}	$Q_{p,out}$	h_{max}	Clogging Rate
Initial Jam	0 1.5 3	[m]	-*	-*	+*	+*
Peak Flow	100 142 250	[m ³ /s]	-*	+*	+*	+*
Deposition Slope	4 8 11	[%]	-*	-*	-*	-*
Time to Peak	3 14 42	[%]	+	+*	+	-
Event Volume	24 80 150	[1000 m ³]	+*	+*	+*	+*
Boulder Composition	0.4 1.1 3.4	[%]	-*	-*	+*	+*
Mixing Volume	0 56 560 5600	[m ³]	-*	-	+*	+*

The results presented in Figure 16 and Table 6 aligned with expectations, and can be explained as follows:

- The greater the initial jam in the structure, the smaller the outflow volume and peak outflow, and the greater the maximum flow level and clogging rate. This is likely because the initial jam mechanically controls the outlet, causing deposition. If more volume is stored (because the clogging rate is higher), less volume flows out of the structure, the peak flow is smaller, and the maximum flow elevation is increased.
- Increasing the peak inflow reduces the outflow volume, likely because more boulders are conveyed through the opening at the same time, encouraging jamming (and therefore deposition). Increasing the peak inflow increases the clogging rate, and therefore also increases the peak outflow and the maximum flow elevation.
- Increasing the deposition slope decreases the outflow volume and peak outflow because a steeper deposition slope allows more volume to be stored behind any jams. This increased storage/decreased debris flow volume also decreases the clogging rate and the maximum flow elevation.
- Increasing the time to peak seems to very slightly increase outflow volume and peak outflow, possibly because fewer boulders were concentrated at the front of the surge, and were, therefore, less likely to jam. Although the relationship between time to peak and peak outflow was found to be statistically significant ($p \ll 0.05$), the correlation between time to peak and outflow volume, maximum flow elevation, and clogging rate was not ($p \gg 0.05$). This indicates that the model results are not highly sensitive to the inputted time to peak value.
- Increasing the volume of the event increases the outflow volume, peak outflow, maximum flow level, and clogging rate. This is likely because although a greater event volume will result in more boulders and therefore more jamming, it also (by definition) results in more volume passing through the structure.
- Increasing the number of boulders decreases the outflow volume and peak outflow, but increases the maximum flow elevation, and the clogging rate. This is likely because more boulders result in more jamming, and therefore more deposition.
- Changing the transfer method from instantaneous to mixing, and increasing the mixing volume did not have a statistically significant effect on the peak outflow, and had less than a 12% difference on the outflow volume. This indicates that the model is robust, and not highly sensitive to the stochastic re-generation of boulders, or uncertainty regarding the transfer type and mixing volume. This is good news because this parameter is difficult to constrain due to

the poor knowledge available on how boulders move and circulate while debris flows erode and deposit in channels and basins. Considering the weak correlation between the mixing volume and the model output, we suggest using an instantaneous transfer hypothesis for preliminary analyses and testing the model sensitivity in uncertainty propagation at later study stages.

4 Discussion

4.1 2005 Event

The Upper Debris Basin jammed in most simulations, attenuating part of the debris flow. The Lower Debris Basin and Upper Bridge also jammed in some scenarios, and generally attenuated less debris than the Upper Debris Basin. These results align with the general historical behaviour of this series of structures.

The jamming heights and deposition volumes recorded following the 2005 event at the Lower Debris Basin and Upper Bridge all fell within the range of results produced by the possibilistic simulation. The model tended to overestimate jamming height and stored volume, meaning that the historical values fell within the lower range of simulated values, rather than at the mean (Figures 15). This can be explained in three ways:

1. Although statistics are often used to predict the most probable outcome of an event, the universe is fundamentally chaotic, and in reality, the most probable outcome does not always occur. For example, even though the simulation results indicate that the 2005 event was likely to cause jamming in the Lower Debris Basin, no jamming was also a possibility, and in reality, was the outcome (**office_national_de_forets_etude_2013.**)
2. The updated framework does not account for transient jamming, a phenomenon that is sometimes observed during debris flows (Marchelli et al., 2020; Choi et al., 2016; Zhou et al., 2020), and is discussed further in Appendix F. It is possible that during the 2005 event, structures were temporarily jammed before the debris was re-mobilized, which would bring the historically recorded jamming height (and therefore deposition) closer to the mean of the model results.
3. It is possible that we overestimated the proportion of the debris flow event composed of 2-3 m boulders. Channel armoring effects make it difficult to accurately estimate the proportion of boulders present during a debris flow event. As well, the quantity and distribution of boulders present in a debris flow varies between events, depending on both debris availability, and the size of the event. The quantity of 2-3 m boulders had a large impact on modeled jamming, and yet is a difficult parameter to constrain. Since jamming tended to be overestimated at both the Upper Debris Basin and the Lower Debris Basin in comparison to the historical records, this explanation is likely.

The last explanation is likely the most significant. It would be possible to define numbers of boulders of the various classes that would result in more consistent jamming probability, thus performing a detailed calibration. We however chose to use a boulder distribution that was determined largely based on field observations in the channel, and in records of previous large debris flow events (i.e. how many boulders larger than 3 m could be found in the deposit). This is thus rather a sort of validation of the model but also an example of the kind of variability that should be expected in the model results when applied in realistic conditions, i.e. without decades of historical records in an existing structure.

As discussed in Section 2.1.3, the Upper Bridge was damaged during the 2005 event. There is uncertainty surrounding the means of destruction - it may have occurred as a result of jamming

and/or overtopping. Both causes of destruction fall within the range of results produced by the possibilistic simulation.

Overall, the model results generally aligned with the historically recorded jamming height and deposition volume. The model's ability to recreate a known event validates its ability to simulate jamming in a cascading series of constrictions.

4.2 Parametric Analysis

The positive/negative correlations between the input variables and the model results (Table 6) were used to define the monotony within the updated framework. Going forward, the monotony of each input variable (Table 6) will be applied to simulations to decrease the possibilistic analysis runtime.

4.3 Limitations and Future Directions

There are several limitations to the model framework presented within this report, which may be addressed as part of future scopes of work. These limitations and future directions are outlined within Appendix F.

5 Conclusion

The Piton et al., 2022 framework was extended to possibilistically simulate jamming during a debris flow event through a series of cascading constrictions. In this study, we applied the extended framework to the Torrent du Saint-Martin, and conducted a parametric analysis of the input variables.

The input parameters required to model the Torrent du Saint-Martin were developed from literature, historical records, a site visit, and expert judgment. All values are summarized in Section 3.

We possibilistically simulated the 2005 debris flow event through three consecutive structures along the Torrent du Saint-Martin's alluvial fan: the Upper Debris Basin, the Lower Debris Basin, and the Upper Bridge (Figure 2). The model results aligned with the historically recorded jamming height and deposition volume (ONF-RTM, 2023). This validates the use of the extended framework to simulate jamming on the Torrent du Saint-Martin.

We also conducted a parametric analysis, to determine the monotony of the input variables, and the model's sensitivity. The variation of all input parameters except the event volume and peak inflow had a limited impact on the model results, varying the mean outflow volume, and peak outflow by 15% or less. The monotony of the various input parameters as determined through the parametric analysis aligned with expectations, and was incorporated into the model framework to reduce model runtime.

Overall, the results of the analyses indicate that the model can be effectively used to simulate jamming caused by a debris flow through a series of debris basins or bridges.

References

- Aaron, J., R. Spielmann, B. W. McARDell, and C. Graf (Mar. 2023). “High-Frequency 3D LiDAR Measurements of a Debris Flow: A Novel Method to Investigate the Dynamics of Full-Scale Events in the Field”. en. In: *Geophysical Research Letters* 50.5, e2022GL102373. ISSN: 0094-8276, 1944-8007. DOI: 10.1029/2022GL102373. URL: <https://agupubs.onlinelibrary.wiley.com/doi/10.1029/2022GL102373> (visited on 05/02/2024).
- Arai, M., J. Huebl, and R. Kaitna (Nov. 2014). “A Wave Equation of Intermittent Flow with Sediment on Inclined Channel and Experimental and Observed Results”. In: *Proceedings of the INTERPRAEVENT 2014 in the Pacific Rim*, pp. 617–624. URL: https://www.interpraevent.at/palm-cms/upload_files/Publikationen/Tagungsbeitraege/2014_1_617.pdf.
- Arattano, M., L. Marchi, and M. Cavalli (Mar. 2012). “Analysis of debris-flow recordings in an instrumented basin: confirmations and new findings”. en. In: *Natural Hazards and Earth System Sciences* 12.3, pp. 679–686. ISSN: 1684-9981. DOI: 10.5194/nhess-12-679-2012. URL: <https://nhess.copernicus.org/articles/12/679/2012/> (visited on 05/13/2024).
- Arattano, M., V. Coviello, C. Abancó, M. Hürlimann, and B. W. McARDELL (2016). “Methods of Data Processing for Debris Flow Seismic Warning”. en. In: *International Journal of Erosion Control Engineering* 9.3, pp. 114–121. ISSN: 1882-6547. DOI: 10.13101/ijece.9.114. URL: https://www.jstage.jst.go.jp/article/ijece/9/3/9_114/_article (visited on 05/13/2024).
- Arattano, M. and L. Marchi (Apr. 2008). “Systems and Sensors for Debris-flow Monitoring and Warning”. en. In: *Sensors* 8.4, pp. 2436–2452. ISSN: 1424-8220. DOI: 10.3390/s8042436. URL: <http://www.mdpi.com/1424-8220/8/4/2436> (visited on 04/29/2024).
- Barbini, M., M. Bernard, M. Boreggio, M. Schiavo, V. D’Agostino, and C. Gregoretti (July 2024). “An alternative approach for the sediment control of in-channel stony debris flows with an application to the case study of Ru Secco Creek (Venetian Dolomites, Northeast Italy)”. In: *Frontiers in Earth Science* 12, p. 1340561. ISSN: 2296-6463. DOI: 10.3389/feart.2024.1340561. URL: <https://www.frontiersin.org/articles/10.3389/feart.2024.1340561/full> (visited on 07/15/2024).
- Bernard, M. and C. Gregoretti (Mar. 2021). “The Use of Rain Gauge Measurements and Radar Data for the Model-Based Prediction of Runoff-Generated Debris-Flow Occurrence in Early Warning Systems”. en. In: *Water Resources Research* 57.3, e2020WR027893. ISSN: 0043-1397, 1944-7973. DOI: 10.1029/2020WR027893. URL: <https://agupubs.onlinelibrary.wiley.com/doi/10.1029/2020WR027893> (visited on 07/15/2024).
- Berti, M., R. Genevois, R. LaHusen, A. Simoni, and P. Tecca (Jan. 2000). “Debris flow monitoring in the acquabona watershed on the Dolomites (Italian alps)”. en. In: *Physics and Chemistry of the Earth, Part B: Hydrology, Oceans and Atmosphere* 25.9, pp. 707–715. ISSN: 14641909. DOI: 10.1016/S1464-1909(00)00090-3. URL: <https://linkinghub.elsevier.com/retrieve/pii/S1464190900000903> (visited on 05/14/2024).
- Bovis, M. J. and M. Jakob (Oct. 1999). “The role of debris supply conditions in predicting debris flow activity”. en. In: *Earth Surface Processes and Landforms* 24.11, pp. 1039–1054. ISSN: 0197-9337, 1096-9837. DOI: 10.1002/(SICI)1096-9837(199910)24:11<1039::AID-ESP29>3.0.CO;2-U. URL: [https://onlinelibrary.wiley.com/doi/10.1002/\(SICI\)1096-9837\(199910\)24:11<1039::AID-ESP29>3.0.CO;2-U](https://onlinelibrary.wiley.com/doi/10.1002/(SICI)1096-9837(199910)24:11<1039::AID-ESP29>3.0.CO;2-U) (visited on 05/17/2024).
- Canelas, R. B., J. M. Domínguez, A. J. C. Crespo, M. Gómez-Gesteira, and R. M. L. Ferreira (Sept. 2017). “Resolved Simulation of a Granular-Fluid Flow with a Coupled SPH-DCDEM Model”. en. In: *Journal of Hydraulic Engineering* 143.9, p. 06017012. ISSN: 0733-9429, 1943-7900. DOI: 10.1061/(ASCE)HY.1943-7900.0001331. URL: <https://ascelibrary.org/doi/10.1061/%28ASCE%29HY.1943-7900.0001331> (visited on 03/14/2024).
- Carladous, S., G. Piton, D. Kuss, G. Charvet, R. Paulhe, M. Morel, and Y. Quefféléan (2022). *Check dam construction for sustainable watershed management and planning*. eng. Ed. by Z. Li, P. Li, Y. Yu, P. Shi, and G. Piton. First edition. Hoboken, NJ: Wiley, pp. 247–266. ISBN: 978-1-119-74240-1.
- Chen, J., D. Wang, W. Zhao, H. Chen, T. Wang, N. Nepal, and X. Chen (July 2020). “Laboratory study on the characteristics of large wood and debris flow processes at slit-check dams”. en. In: *Landslides* 17.7, pp. 1703–1711. ISSN: 1612-510X, 1612-5118. DOI: 10.1007/s10346-020-01409-3. URL: <https://link.springer.com/10.1007/s10346-020-01409-3> (visited on 05/02/2024).
- Choi, C. E., G. R. Goodwin, C. W. W. Ng, D. K. H. Cheung, J. S. H. Kwan, and W. K. Pun (Dec. 2016). “Coarse granular flow interaction with slit structures”. en. In: *Géotechnique Letters* 6.4, pp. 267–274. ISSN:

- 2045-2543. DOI: 10.1680/jgele.16.00103. URL: <https://www.icevirtuallibrary.com/doi/10.1680/jgele.16.00103> (visited on 05/02/2024).
- Coviello, V. (Apr. 2015). “Debris flow seismic monitoring and warning”. English. PhD Thesis. Torino: Politecnico Di Torino. URL: <https://core.ac.uk/download/pdf/76527626.pdf>.
- Coviello, V., J. I. Theule, S. Crema, M. Arattano, F. Comiti, M. Cavalli, A. Lucía, P. Macconi, and L. Marchi (Feb. 2021). “Combining Instrumental Monitoring and High-Resolution Topography for Estimating Sediment Yield in a Debris-Flow Catchment”. en. In: *Environmental and Engineering Geoscience* 27.1, pp. 95–111. ISSN: 1078-7275. DOI: 10.2113/EEG-D-20-00025. URL: <https://pubs.geoscienceworld.org/aeg/eeg/article/27/1/95/595099/Combining-Instrumental-Monitoring-and-High> (visited on 04/29/2024).
- Dong, L. and J. Pu (Feb. 2024). “Debris–slit interaction considering the particle behavior controls the barrier performance of slit structure retaining dry granular flows”. en. In: *Environmental Earth Sciences* 83.3, p. 107. ISSN: 1866-6280, 1866-6299. DOI: 10.1007/s12665-023-11323-1. URL: <https://link.springer.com/10.1007/s12665-023-11323-1> (visited on 05/02/2024).
- Fenske, T. E., C. J. Apelt, and A. C. Parola (1995). “Debris forces and impact on highway bridges”. In: Medium: text/html,application/pdf,text/html Publisher: [object Object]. DOI: 10.5169/SEALS-55304. URL: <https://www.e-periodica.ch/digbib/view?pid=bse-re-003:1995:73/1:73/2::1193> (visited on 04/29/2024).
- Friedl, C., C. Scheidl, S. Wernhart, and D. Proske (June 2024). “Assessing Granular Debris-Flow Impact Forces on Bridge Superstructures”. en. In: *Journal of Bridge Engineering* 29.6, p. 04024027. ISSN: 1084-0702, 1943-5592. DOI: 10.1061/JBENF2.BEENG-6439. URL: <https://ascelibrary.org/doi/10.1061/JBENF2.BEENG-6439> (visited on 04/29/2024).
- Goodwin, S. and C. Choi (Mar. 2020). “Slit structures: Fundamental mechanisms of mechanical trapping of granular flows”. en. In: *Computers and Geotechnics* 119, p. 103376. ISSN: 0266352X. DOI: 10.1016/j.compgeo.2019.103376. URL: <https://linkinghub.elsevier.com/retrieve/pii/S0266352X19304409> (visited on 05/02/2024).
- Gregoretto, C., L. M. Stancanelli, M. Bernard, M. Boreggio, M. Degetto, and S. Lanzoni (Jan. 2019). “Relevance of erosion processes when modelling in-channel gravel debris flows for efficient hazard assessment”. en. In: *Journal of Hydrology* 568, pp. 575–591. ISSN: 00221694. DOI: 10.1016/j.jhydrol.2018.10.001. URL: <https://linkinghub.elsevier.com/retrieve/pii/S0022169418307625> (visited on 07/15/2024).
- Hengbin Wu, Na He, and Xuefu Zhang (Jan. 2015). “Numerical Model of Viscous Debris Flows with Depth-Dependent Yield Strength”. en. In: *Journal of GeoEngineering* 10.1. DOI: 10.6310/jog.2015.10(1).1.
- Horiguchi, T., G. Piton, M. Munir, and V. Mano (June 2021). “Driftwood and Hybrid Debris Barrier Interactions: Process of Trapping and Prevention of Releases during Overtopping”. In.
- Hugerot, T. (May 2016). “Trajectoires socio-environmentales des cônes de déjection torrentiels en vallée de Maurienne depuis la fin du Petit Âge Glaciaire”. French. PhD thesis. Université Savoie Mont Blanc.
- Hungr, O., G. Morgan, and R. Kellerhals (1984). “Quantitative analysis of debris torrent hazards for design of remedial measures.” In: *Canadian Geotechnical Journal* 21.4, pp. 663–677. ISSN: 00083674. DOI: 10.1139/t84-073.
- Ikeda, A., T. Mizuyama, and T. Itoh (2019). “Study of prediction methods of debris-flow peak discharge”. In.
- Jempson, M. (Mar. 2000). “Flood and Debris Loads on Bridges”. PhD Thesis. University of Queensland. URL: <https://espace.library.uq.edu.au/view/UQ:206022>.
- Lapillonne, S., F. Fontaine, F. Liebault, V. Richefeu, and G. Piton (Apr. 2023). “Debris-flow surges of a very active alpine torrent: a field database”. en. In: *Natural Hazards and Earth System Sciences* 23.4, pp. 1241–1256. ISSN: 1684-9981. DOI: 10.5194/nhess-23-1241-2023. URL: <https://nhess.copernicus.org/articles/23/1241/2023/> (visited on 05/13/2024).
- Marchelli, M., A. Leonardi, M. Pirulli, and C. Scavia (Mar. 2020). “On the efficiency of slit-check dams in retaining granular flows”. en. In: *Géotechnique* 70.3, pp. 226–237. ISSN: 0016-8505, 1751-7656. DOI: 10.1680/jgeot.18.P.044. URL: <https://www.icevirtuallibrary.com/doi/10.1680/jgeot.18.P.044> (visited on 05/03/2024).
- Marchi, L., F. Cazorzi, M. Arattano, S. Cucchiario, M. Cavalli, and S. Crema (Jan. 2021). “Debris flows recorded in the Moscardo catchment (Italian Alps) between 1990 and 2019”. en. In: *Natural Hazards and Earth System Sciences* 21.1, pp. 87–97. ISSN: 1684-9981. DOI: 10.5194/nhess-21-87-2021. URL: <https://nhess.copernicus.org/articles/21/87/2021/> (visited on 04/26/2024).
- Mitchell, A., S. Zubrycky, S. McDougall, J. Aaron, M. Jacquemart, J. Hübl, R. Kaitna, and C. Graf (May 2022). “Variable hydrograph inputs for a numerical debris-flow runout model”. en. In: *Natural Hazards and*

- Earth System Sciences* 22.5, pp. 1627–1654. ISSN: 1684-9981. DOI: 10.5194/nhess-22-1627-2022. URL: <https://nhess.copernicus.org/articles/22/1627/2022/> (visited on 04/26/2024).
- Mizuyama, T., S Kobashi, and G Ou (1992). “Prediction of Debris Flow Peak Discharge”. In: *Internationales Symposium*. Bern, pp. 99–108. URL: https://www.interpraevent.at/palm-cms/upload_files/Publikationen/Tagungsbeitraege/1992_4_99.pdf.
- Nagl, G., J. Hübl, and R. Kaitna (June 2020). “Velocity profiles and basal stresses in natural debris flows”. en. In: *Earth Surface Processes and Landforms* 45.8, pp. 1764–1776. ISSN: 0197-9337, 1096-9837. DOI: 10.1002/esp.4844. URL: <https://onlinelibrary.wiley.com/doi/10.1002/esp.4844> (visited on 04/29/2024).
- Nakatani, K., S. Hayami, Y. Satofuka, and T. Mizuyama (Feb. 2016). “Case study of debris flow disaster scenario caused by torrential rain on Kiyomizu-dera, Kyoto, Japan - using Hyper KANAKO system”. en. In: *Journal of Mountain Science* 13.2, pp. 193–202. ISSN: 1672-6316, 1993-0321. DOI: 10.1007/s11629-015-3517-7. URL: <http://link.springer.com/10.1007/s11629-015-3517-7> (visited on 03/14/2024).
- Navratil, O., F. Liébault, H. Bellot, J. Theule, E. Travaglini, J.-L. Demirdjian, X. Ravanat, F. Ousset, D. Laigle, V. Segel, and M. Fiquet (Jan. 2012). “High-frequency monitoring of debris flows in the French Alps: preliminary results of a starting program”. In.
- ONF-RTM (July 2013). *Etude de bassin versant Torrent du Saint-Martin*. Tech. rep. Office National de Forêts - Service de Restauration des Terrains de Montagne, pp. 6–125.
- (2023). *Dossier d'autorisation du système d'endiguement du Saint-Martin : Etude de danger*. Tech. rep. Office National de Forêts and Restauration des terrains en montagne.
- Oudenbroek, K., N. Naderi, J. Bricker, Y. Yang, C. van der Veen, W. Uijttewaal, S. Moriguchi, and S. Jonkman (Nov. 2018). “Hydrodynamic and Debris-Damming Failure of Bridge Decks and Piers in Steady Flow”. en. In: *Geosciences* 8.11, p. 409. ISSN: 2076-3263. DOI: 10.3390/geosciences8110409. URL: <http://www.mdpi.com/2076-3263/8/11/409> (visited on 04/29/2024).
- Piton, G. and A. Recking (2016). “Design of sediment traps with open check dams. I: hydraulic and deposition processes”. In: *Journal of Hydraulic Engineering* 142.2, pp. 1–23. DOI: 10.1061/(ASCE)HY.1943-7900.0001048.
- Piton, G., G. Charvet, D. Kuss, and S. Carladou (June 2020). “Putting a Grill (or Not) in Slit Dams Aiming at Trapping Debris Flows? Lessons Learnt From France”. In: 1, pp. 1–5.
- Piton, G., V. D’agnostino, T. Horiguchi, A. Ikeda, and J. Hübl (2024). “Functional Design of Mitigation Measures: From Design Event Definition to Targeted Process Modifications”. In: *Advances in Debris-flow Science and Practice*. Geoenvironmental Disaster Reduction. ISBN: 978-3-031-48691-3.
- Piton, G., S. R. Goodwin, E. Mark, and A. Strouth (May 2022). “Debris Flows, Boulders and Constrictions: A Simple Framework for Modeling Jamming, and Its Consequences on Outflow”. en. In: *Journal of Geophysical Research: Earth Surface* 127.5, e2021JF006447. ISSN: 2169-9003, 2169-9011. DOI: 10.1029/2021JF006447. URL: <https://agupubs.onlinelibrary.wiley.com/doi/10.1029/2021JF006447> (visited on 03/07/2024).
- Raffaele Spielmann (Aug. 2022). “Understanding Debris-Flow Motion through Detailed Analysis of Timelapse Point Clouds Collected by High-Frequency 3D LiDAR Scanners Ilgraben, Switzerland”. MA thesis. Zurich: ETH Zurich. URL: https://www.research-collection.ethz.ch/bitstream/handle/20.500.11850/618113/MasterThesis_RaffaeleSpielmann_Final_withPermission.pdf?sequence=1&isAllowed=y.
- Rickenmann, D. (1999). “Empirical Relationships for Debris Flows”. In: *Natural Hazards* 19, pp. 47–77. URL: https://www.dora.lib4ri.ch/wsl/islandora/object/wsl%3A3611/datastream/PDF/Rickenmann-1999-Empirical_relationships_for_debris_flows-%28published_version%29.pdf.
- Rickli, C., A. Badoux, D. Rickenmann, N. Steeb, and P. Waldner (Mar. 2018). “Large wood potential, piece characteristics, and flood effects in Swiss mountain streams”. en. In: *Physical Geography*, pp. 1–23. ISSN: 0272-3646, 1930-0557. DOI: 10.1080/02723646.2018.1456310. URL: <https://www.tandfonline.com/doi/full/10.1080/02723646.2018.1456310> (visited on 05/03/2024).
- Rohmer, J., manceau, Guyonnet, Boulahya, and Dubois (Aug. 2018). *HYRISK: An R package for hybrid uncertainty analysis using probability, imprecise probability and possibility distributions*. preprint. Engineering. DOI: 10.31223/OSF.IO/J67CY. URL: <https://eartharxiv.org/repository/view/1236> (visited on 03/19/2024).
- RTM (n.d.). *Archives of the Restauration des Terrains de Montagne in Chambéry*.
- Schimmel, A., V. Coviello, and F. Comiti (June 2022). “Debris flow velocity and volume estimations based on seismic data”. en. In: *Natural Hazards and Earth System Sciences* 22.6, pp. 1955–1968. ISSN: 1684-9981. DOI: 10.5194/nhess-22-1955-2022. URL: <https://nhess.copernicus.org/articles/22/1955/2022/> (visited on 05/13/2024).

- Schöffl, T., G. Nagl, R. Koschuch, H. Schreiber, J. Hübl, and R. Kaitna (Sept. 2023). “A Perspective of Surge Dynamics in Natural Debris Flows Through Pulse-Doppler Radar Observations”. en. In: *Journal of Geophysical Research: Earth Surface* 128.9, e2023JF007171. ISSN: 2169-9003, 2169-9011. DOI: 10.1029/2023JF007171.
- Simoni, A., M. Bernard, M. Berti, M. Boreggio, S. Lanzoni, L. M. Stancanelli, and C. Gregoret (Nov. 2020). “Runoff-generated debris flows: Observation of initiation conditions and erosion–deposition dynamics along the channel at Cancia (eastern Italian Alps)”. en. In: *Earth Surface Processes and Landforms* 45.14, pp. 3556–3571. ISSN: 0197-9337, 1096-9837. DOI: 10.1002/esp.4981. URL: <https://onlinelibrary.wiley.com/doi/10.1002/esp.4981> (visited on 05/02/2024).
- Sun, H., Y. You, and J. Liu (Dec. 2018). “Experimental study on blocking and self-cleaning behaviors of beam dam in debris flow hazard mitigation”. en. In: *International Journal of Sediment Research* 33.4, pp. 395–405. ISSN: 10016279. DOI: 10.1016/j.ijsrc.2018.04.004. URL: <https://linkinghub.elsevier.com/retrieve/pii/S1001627917302731> (visited on 03/07/2024).
- Swartz, M., B. McArdeell, P. Bartelt, and M. Christen (2004). “EVALUATION OF A TWO-PHASE DEBRIS FLOW MODEL USING FIELD DATA FROM THE SWISS ALPS”. In: *Internationales Symposium. Riva/Trient*, pp. 319–329.
- Theule, J., F. Liébault, D. Laigle, A. Loye, and M. Jaboyedoff (2015). “Channel scour and fill by debris flows and bedload transport”. In: *Geomorphology* 243, pp. 92–105. ISSN: 0169555X. DOI: 10.1016/j.geomorph.2015.05.003.
- Torresani, L., G. Piton, and V. D’Agostino (2023). “Morphodynamics and Sediment Connectivity Index in an unmanaged, debris-flow prone catchment: a new perspective”. In: *Journal of Mountain Science* 20.4, pp. 891–910. DOI: 10.1007/s11629-022-7746-2.
- Wang, D., X. Wang, X. Chen, B. Lian, and J. Wang (Feb. 2022a). “Analysis of factors influencing the large wood transport and block-outburst in debris flow based on physical model experiment”. en. In: *Geomorphology* 398, p. 108054. ISSN: 0169555X. DOI: 10.1016/j.geomorph.2021.108054. URL: <https://linkinghub.elsevier.com/retrieve/pii/S0169555X21004621> (visited on 05/02/2024).
- Wang, D., X. Wang, X. Chen, B. Lian, J. Wang, and F. Wang (Sept. 2022b). “Laboratory flume experiments on the characteristics of large wood accumulations from debris flow and the backwater rise at slit-check dams”. en. In: *Landslides* 19.9, pp. 2135–2148. ISSN: 1612-510X, 1612-5118. DOI: 10.1007/s10346-022-01887-7. URL: <https://link.springer.com/10.1007/s10346-022-01887-7> (visited on 05/02/2024).
- Wang, D., Z. Chen, S. He, Y. Liu, and H. Tang (July 2018). “Measuring and estimating the impact pressure of debris flows on bridge piers based on large-scale laboratory experiments”. en. In: *Landslides* 15.7, pp. 1331–1345. ISSN: 1612-510X, 1612-5118. DOI: 10.1007/s10346-018-0944-x. URL: <http://link.springer.com/10.1007/s10346-018-0944-x> (visited on 04/29/2024).
- Xia, C. and H. Tian (Apr. 2022). “A Quasi-Single-Phase Model for Debris Flows Incorporating Non-Newtonian Fluid Behavior”. en. In: *Water* 14.9, p. 1369. ISSN: 2073-4441. DOI: 10.3390/w14091369. URL: <https://www.mdpi.com/2073-4441/14/9/1369> (visited on 05/07/2024).
- Xie, X., X. Wang, Z. Liu, Z. Liu, and S. Zhao (Jan. 2023). “Regulation effect of slit-check dam against woody debris flow: Laboratory test”. In: *Frontiers in Earth Science* 10, p. 1023652. ISSN: 2296-6463. DOI: 10.3389/feart.2022.1023652. URL: <https://www.frontiersin.org/articles/10.3389/feart.2022.1023652/full> (visited on 05/02/2024).
- Xiong, M., X. Meng, S. Wang, P. Guo, Y. Li, G. Chen, F. Qing, Z. Cui, and Y. Zhao (Dec. 2016). “Effectiveness of debris flow mitigation strategies in mountainous regions”. en. In: *Progress in Physical Geography: Earth and Environment* 40.6, pp. 768–793. ISSN: 0309-1333, 1477-0296. DOI: 10.1177/0309133316655304. URL: <http://journals.sagepub.com/doi/10.1177/0309133316655304> (visited on 03/07/2024).
- Yuan, D., J. Liu, Y. You, G. Zhang, D. Wang, and Z. Lin (Dec. 2019). “Experimental study on the performance characteristics of viscous debris flows with a grid-type dam for debris flow hazards mitigation”. en. In: *Bulletin of Engineering Geology and the Environment* 78.8, pp. 5763–5774. ISSN: 1435-9529, 1435-9537. DOI: 10.1007/s10064-019-01524-z. URL: <http://link.springer.com/10.1007/s10064-019-01524-z> (visited on 03/11/2024).
- Zhou, G. G. D., J. Du, D. Song, C. E. Choi, H. S. Hu, and C. Jiang (Mar. 2020). “Numerical study of granular debris flow run-up against slit dams by discrete element method”. en. In: *Landslides* 17.3, pp. 585–595. ISSN: 1612-510X, 1612-5118. DOI: 10.1007/s10346-019-01287-4. URL: <http://link.springer.com/10.1007/s10346-019-01287-4> (visited on 05/06/2024).
- Zuriguél, I., A. Garcimartín, D. Maza, L. A. Pagnaloni, and J. M. Pastor (May 2005). “Jamming during the discharge of granular matter from a silo”. en. In: *Physical Review E* 71.5, p. 051303. ISSN: 1539-3755, 1550-

2376. DOI: 10.1103/PhysRevE.71.051303. URL: <https://link.aps.org/doi/10.1103/PhysRevE.71.051303> (visited on 05/07/2024).

A Structural Mitigations of the Torrent du Saint-Martin

There are many types of protection works along the Torrent du Saint-Martin, including slope stabilization works (i.e. drains and re-vegetation efforts), as well as in-channel works, such as debris basins, check dams, and a conveyance channel (Hugerot, 2016). An overview of current mitigation measures within the channel is shown in Figure 2.

Mitigations Upstream of the Alluvial Fan Many of the mitigations within the Torrent du Saint-Martin are upstream of the alluvial fan. Some are no longer actively maintained (Hugerot, 2016; ONF-RTM, 2023). All currently maintained in-channel protection works exist along the Torrent de Benoît (the west tributary channel), or below the confluence of the two main tributary channels (Figure 2) (ONF-RTM, 2023).

Debris flow volumes fluctuate as the event flows downstream due to erosion and deposition, and volumes are typically estimated just upstream of the fan apex. Therefore, only the mitigations within the alluvial fan were explicitly modeled in this study. The mitigation works upstream of the alluvial fan change the morphology of the channel, moderating the characteristics of historical debris flows, and are therefore intrinsically accounted for in the ONF-RTM, 2013 Frequency-Magnitude estimates (Table 1).

B General Updates to Model Framework

In addition to the extension of the framework to allow modeling of debris flows through a series of structures and through bridges, several general adjustments were made to the Piton et al. (2022) framework, including:

- An adjustment to the weir equation so a weir with vertical walls above its crest (Figure 17) can be modeled. Previously, this specific opening configuration could not be simulated. A weir that transitions to vertical walls is modeled as a large trapezoidal weir, minus a triangular weir with height above the top level of the inclined wings. The geometry of the calculation is shown in Figure 17. This calculation method is not completely geometrically accurate but produces a reasonable enough approximation for flow calculations.
- If an opening is smaller than the smallest boulder class, it is automatically assumed to be jammed. This is a conservative but necessary assumption, due to the impossibility of accurately estimating the number of boulders present that are smaller than the smallest class.
- In the case of a structure with multiple openings, and in the case of instantaneous transfer, the boulders routed from the upstream structure are randomly distributed between the orifices proportionally to the discharge passing through them.

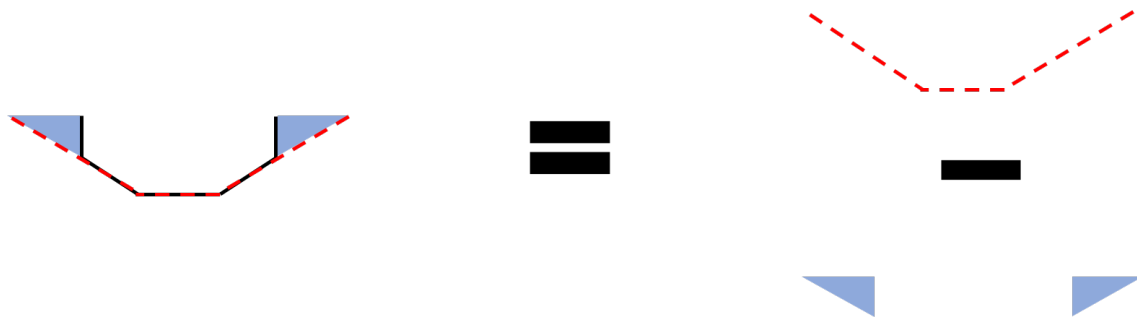


Figure 17: Geometric configuration of calculation for a weir transitioning into vertical walls. The flow through a weir transitioning to vertical walls (shown in black) is calculated by modeling flow through a large trapezoidal weir (shown in dashed red) minus the flow through a triangular weir starting at the level of the vertical side wall (shown in blue).

C Input Parameters

All input parameters used to simulate the 2005 debris flow event are shown in Table 8, 9, 10, 11, 12, 13, 14, 15, 16, and 17.

Table 7: "Events" data used to simulate the 2005 event (1/2). The exceptional event was selected to simulate the 2005 event.

Name	Volume_min	Volume_BestEstimate	Volume_max	PeakDischarge_min	PeakDischarge_BestEstimate	PeakDischarge_max
courant	5000	8000	15000	16	23	37
frequent	9000	30000	36000	50	65	100
rare	24000	80000	150000	100	142	250
exceptional	70000	150000	250000	200	233	350

Table 8: "Events" data used to simulate the 2005 event (2/2). The exceptional event was selected to simulate the 2005 event.

Name	TimeLag_min	TimeLag_BestEstimate	TimeLag_max	DepositionSlope_min	DepositionSlope_BestEstimate	DepositionSlope_max
courant	0.03	0.14	0.42	0.04	0.08	0.11
frequent	0.03	0.14	0.42	0.04	0.08	0.11
rare	0.03	0.14	0.42	0.04	0.08	0.11
exceptional	0.03	0.14	0.42	0.04	0.08	0.11

Table 9: "InitialConditions" data used to simulate the 2005 event.

Name	DepositHeight_min	DepositHeight_BestEstimate	DepositHeight_max	JammingHeight_min	JammingHeight_BestEstimate	JammingHeight_max
Empty	0	0.01	0.02	0	0.01	0.02
1.5 m jam and deposit	1.5	1.51	1.52	1.5	1.51	1.52
3 m jam and deposit	3	3.01	3.02	3	3.01	3.02
1.5 m jam no deposit	0	0.01	0.02	1.5	1.51	1.52
3 m jam no deposit	0	0.01	0.02	3	3.01	3.02

Table 10: "RangeOfBoulders" data used to simulate the 2005 event.

Diameter_min	Diameter_max	Number_BestEstimate	Number_min	Number_max	ReferenceVolume
1	2	5600	2000	16 600	157 500
2	3	280	100	830	157 500
3	4	2	0	10	157 500
4	5	1	0	5	157 500

Table 11: "StructureList" data used to simulate the 2005 event.

Variable	Value
Structure	pdd 1
InitialCondition	Empty
TransferDownstream	Mixing 5600
Structure	pdd 2
InitialCondition	Empty
TransferDownstream	Mixing 5000
Structure	pont 1
InitialCondition	Empty

Table 12: "ElevationStorageCurves" data for the Upper Debris Basin used to simulate the 2005 event.

Z	S0.04	S0.08	S0.11
899	0	0	0
901	59	410	2382
902	548	2003	4935
903	1674	4302	7796
904	3362	6910	10987
905	5523	9797	14523
906	8066	12997	18527
907	10904	16533	23123
908	14038	20511	28364
909	17493	25096	34197
910	21334	30197	40604
911	25740	35714	47796
912	30536	41631	55912
913	35618	47899	64870
914	40907	54498	74371
915	46344	61328	84245

Table 13: "Opening" data for the Upper Debris Basin used to simulate the 2005 event.

Number,Type,Width,BaseLevel,TopLevel,SideAngle,VerticalClogging,LateralClogging
 1,slit,5,899,906.25,90,0,0
 2,slit,8,906.75,906.76,90,0,0
 3,weir,0,908.3,914.3,15,0,0

Table 14: "ElevationStorageCurves" data for the Lower Debris Basin used to simulate the 2005 event.

Z	S0.04	S0.08	S0.11
804.5	0	0	0
807	16	307	3670
808	301	2154	7260
809	1272	4856	11263
810	3046	8327	15738
811	5444	12276	20836
812	8282	16710	26572
813	11685	21623	32932
814	15797	26975	39978
815	20458	32839	47694
816	25632	39377	56066
817	31255	46540	65064
818	37334	54395	74706
819	43917	62946	85003

Table 15: "Opening" data for the Lower Debris Basin used to simulate the 2005 event.

Number,Type,Width,BaseLevel,TopLevel,SideAngle
 1,slit,5,804.5,814.9,90
 2,slit,12,809.3,809.31,90
 3,weir,0,814.9,814.91,10.3

Table 16: "Bridge" data for the Upper Bridge used to simulate the 2005 event.

width slope
 13 0.1


Table 17: "Opening" data for the Upper Bridge used to simulate the 2005 event.

Number,Type,Width,BaseLevel,TopLevel,SideAngle
 1,slot,13,722.5,726.4,90
 2,slit,100,727.5,727.51,90

D Methodology for Volume-Elevation Curve Development


To stochastically simulate jamming of boulders in a constriction during a debris flow using the model framework, a VE curve is required for each deposition basin. The deposition slope is bracketed possibilistically with a user-defined minimum, maximum, and best estimate values. For each of these deposition slopes, a separate VE curve must be computed. The VE curve of a deposition basin with a given deposition slope can be computed using the software Global Mapper. The procedure for using Global Mapper to compute a VE curve is recorded in this Appendix.

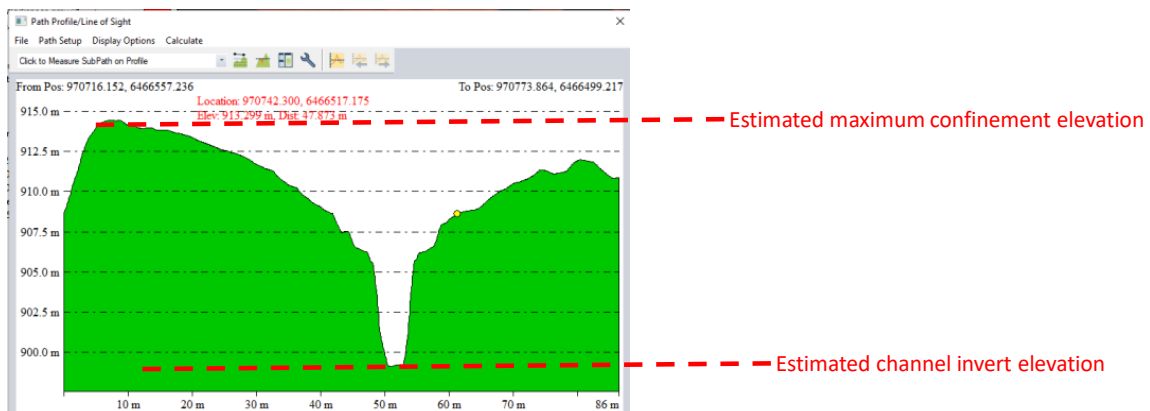
Step 1

- Load Lidar data that completely covers your deposition basin into Global Mapper, by selecting File/Open, or by clicking and dragging the file from the Explorer window into the Global Mapper workspace. 

Page ii



Step 2

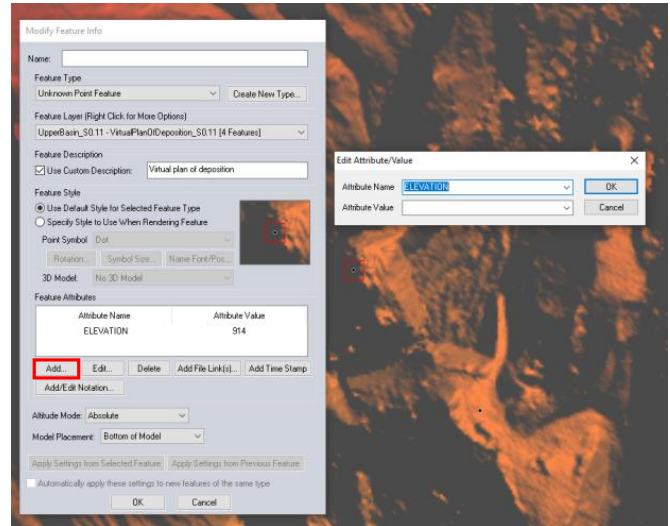
- Locate the deposition basin, and using the Path Profile tool, measure the maximum confinement elevation (i.e. the elevation over which flow overtops the confining structure) 
- Measure the channel invert elevation at the base of the constriction. Note, the channel invert elevation must align with the base elevation defined in the structure's Opening.txt input file.



Page iii

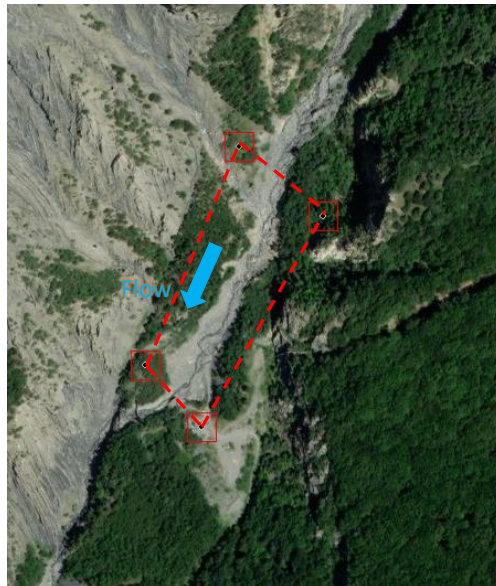
Step 3

- Create four point features, using the Create Point/Text Features tool. 
- The four point features should approximately form a rectangle, encapsulating the deposition basin. The two downstream points should be aligned with the constriction, and their elevation set to the maximum confinement elevation (measured in Step 2).
- The elevation of the two upstream points should be calculated based on their distance from the two downstream points, and the deposition angle (e.g. if the rectangle is 100 m long, and the deposition slope is 10%, the two upstream points should have an elevation that is 10 m higher than that of the two downstream points). They should be set sufficiently far upstream that deposited debris will intercept the topography
 - Adjust the elevation of the points by selecting them with the digitizer tool, right clicking and selecting "EDIT – Edit Point Feature". 
 - In the menu that appears, select "Add" under "Feature Attributes". Enter "ELEVATION" as the Attribute Name, and enter the elevation associated with the feature



Page iv

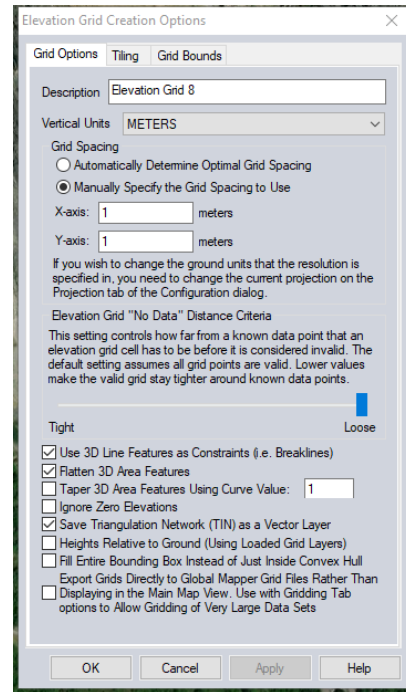
- The rectangle formed by the four point features should be approximately aligned with the direction of deposition (i.e. parallel to the flow direction).



Page v

Step 4

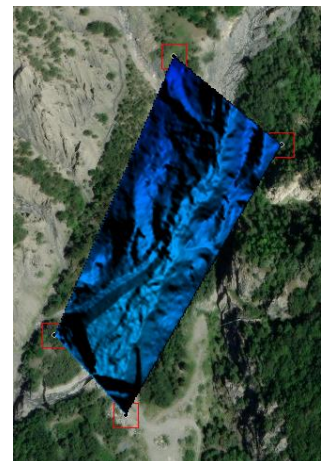
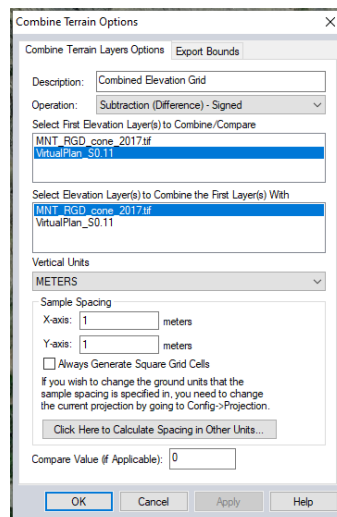
- Using the digitizer tool, select all four point features created in Step 3, and use the Create Elevation Grid tool to create an elevation grid.
 - In the Elevation Grid Creation Options menu that appears, manually specify the grid spacing to be approximately equal to that of the DEM.
 - Select "Save Triangulation Network (TIN) as a Vector Layer



Page vi

Step 5

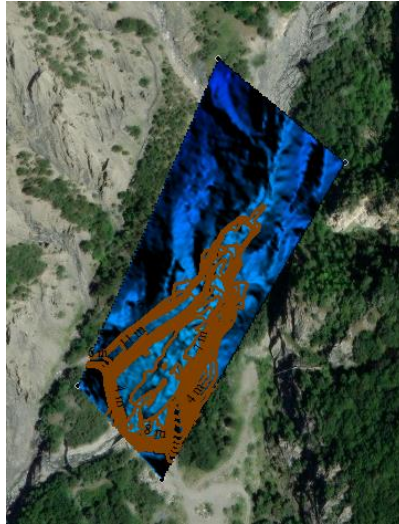
- Using the Combine/Compare Terrain Layers tool, subtract the elevation grid that you created in Step 4 from the DEM.
- The terrain that is produced is the inverse of the bathymetry of the deposition basin.



Page vii

Step 6

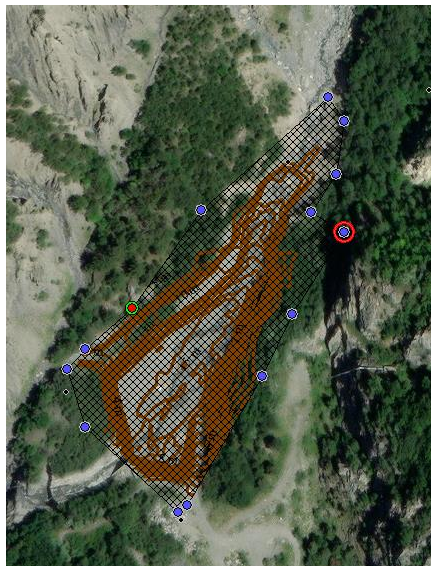
- Using the Create Contours tool, create contours on the DEM created in Step 5 between 0 m and the maximum elevation.



Page viii

Step 7

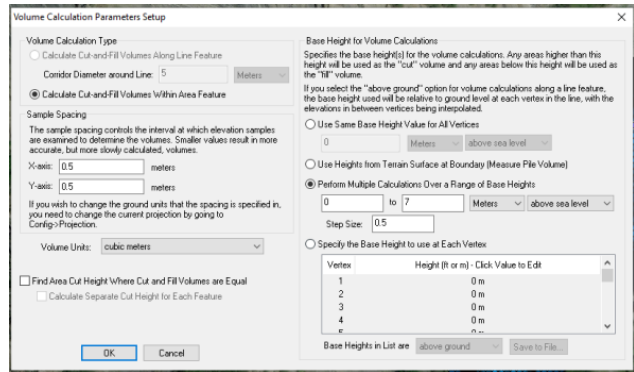
- Using the Create Area Feature tool, approximately outline the contour that follows the edge of the deposition basin.



Page ix

Step 8

- Using the Digitizer Tool, select the area feature created in Step 7.
- With the bathymetry layer produced in Step 5 switched on, select the Calculate Cut and Fill Volume tool.
- In the Volume Calculation Parameters Setup menu that appears, set the sample spacing to be a little less than the resolution of the DEM.
- Select “Perform Multiple Calculations Over a Range of Base Heights”, and click OK.



Step 9

- The Calculated Values that appear at the completion of Step 8 are the VE values. The Base Height column is the elevation relative to the channel invert. Adjust these values to reflect absolute elevation, using the channel invert elevation measured in Step 2.
- The Cut Volume is the deposition volume associated with a given elevation.

BASE_HEIGHT	CUT_VOLUME	CUT_AREA	CUT_AREA_3D	FILL_VOLUME	FILL_AREA	FILL_AREA_3D
0 m	198759.44 cubic meters	0.01016 sq km	0.01981 sq km	806.35403 cubic meters	0.0004627 sq km	0.000643 sq km
0.5 m	193708.73 cubic meters	0.01003 sq km	0.01952 sq km	1068.0384 cubic meters	0.000597 sq km	0.000932 sq km
1 m	188735.52 cubic meters	0.00986 sq km	0.0186 sq km	1407.2182 cubic meters	0.000761 sq km	0.001852 sq km
1.5 m	183855.8 cubic meters	0.00965 sq km	0.01789 sq km	1839.8959 cubic meters	0.000976 sq km	0.002554 sq km
2 m	179091.55 cubic meters	0.0094 sq km	0.01732 sq km	2388.0359 cubic meters	0.001221 sq km	0.003129 sq km
2.5 m	174461.91 cubic meters	0.0091 sq km	0.01668 sq km	3070.7889 cubic meters	0.001522 sq km	0.003772 sq km
3 m	170002.26 cubic meters	0.00872 sq km	0.0155 sq km	3923.5358 cubic meters	0.001901 sq km	0.004945 sq km
3.5 m	165749.88 cubic meters	0.00825 sq km	0.01464 sq km	4983.54 cubic meters	0.002378 sq km	0.00581 sq km
4 m	161758.88 cubic meters	0.00773 sq km	0.01341 sq km	6304.9414 cubic meters	0.002891 sq km	0.00703 sq km
4.5 m	157996.69 cubic meters	0.00732 sq km	0.01266 sq km	7855.1411 cubic meters	0.0033 sq km	0.00779 sq km
5 m	154440.78 cubic meters	0.00689 sq km	0.01169 sq km	9611.6267 cubic meters	0.003738 sq km	0.00875 sq km
5.5 m	151094.38 cubic meters	0.00653 sq km	0.01047 sq km	11577.62 cubic meters	0.0041 sq km	0.00998 sq km
6 m	147906.29 cubic meters	0.00623 sq km	0.00983 sq km	13701.923 cubic meters	0.004393 sq km	0.01062 sq km
6.5 m	144858.59 cubic meters	0.00596 sq km	0.00875 sq km	15966.614 cubic meters	0.004667 sq km	0.0117 sq km
7 m	141949.21 cubic meters	0.00568 sq km	0.00825 sq km	18369.627 cubic meters	0.004943 sq km	0.0122 sq km

Step 10

- Repeat Steps 3-9 for the minimum, maximum, and best estimate deposition slopes.
- Export and save results.

E Model Results

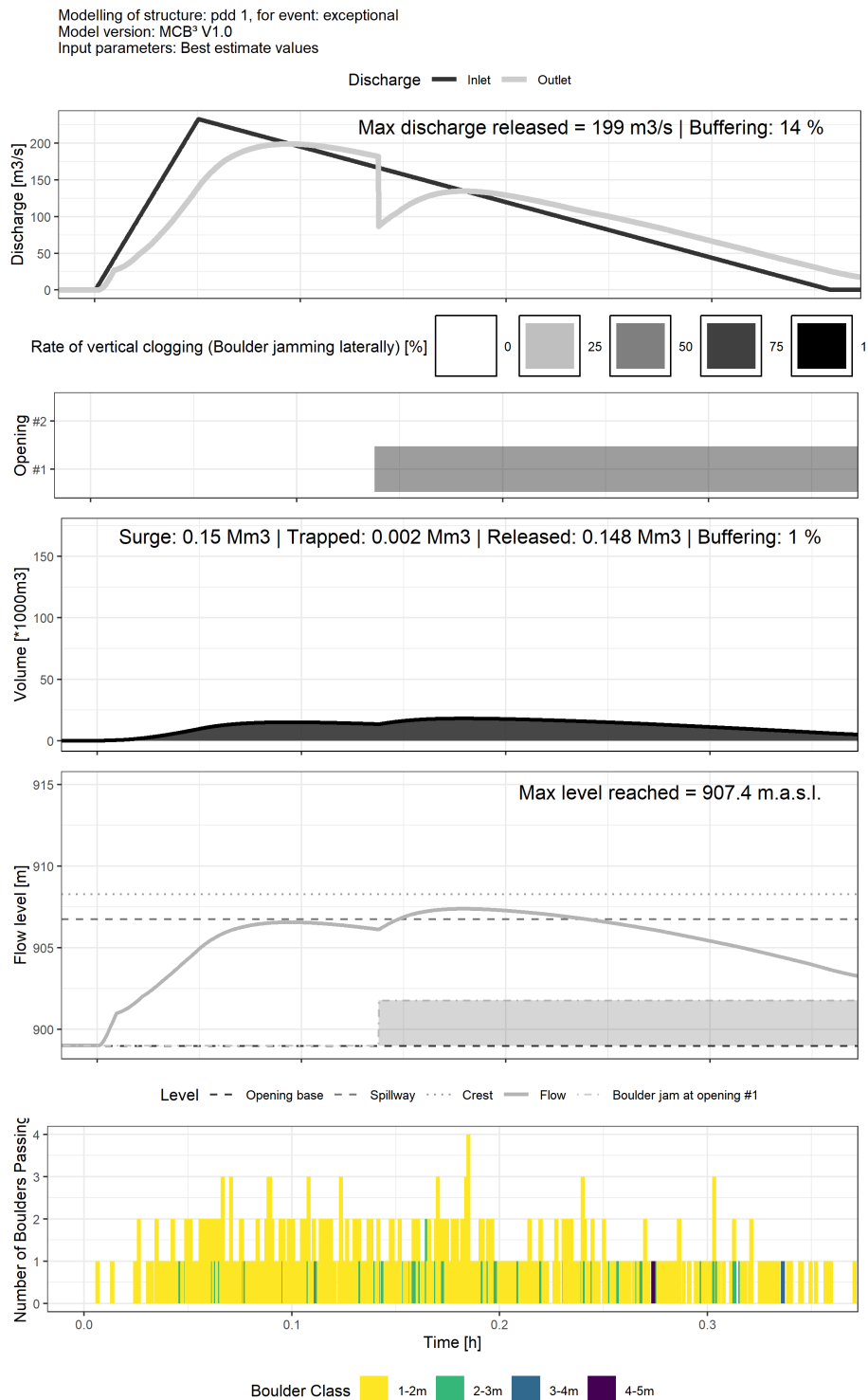


Figure 18: Discharge, clogging, flow level, volume, and generated boulders in the Upper Debris Basin from one “normal” run, simulating the 2005 event.

Modelling Jamming Caused by Debris Flows Through a Series of Cascading Structures

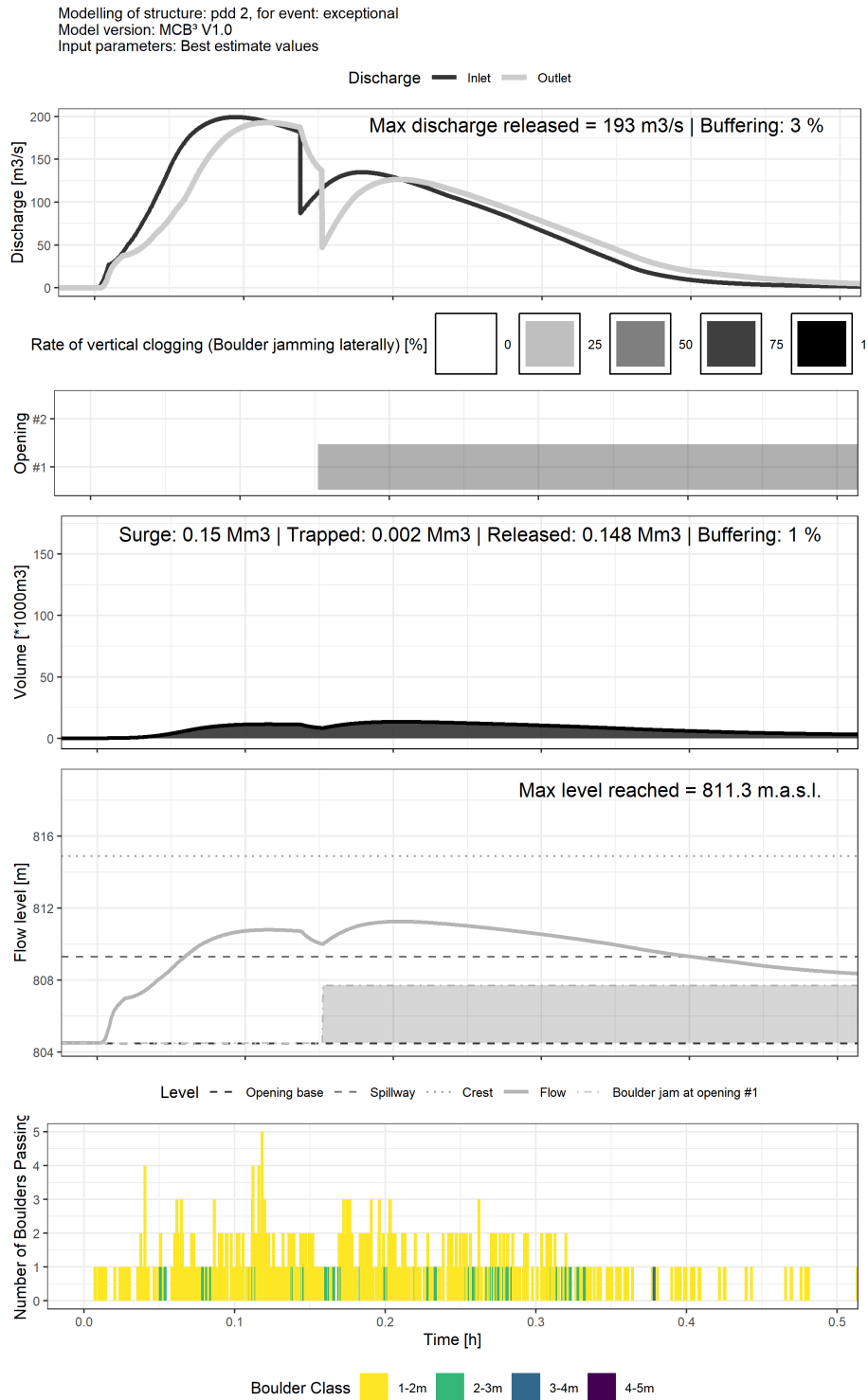


Figure 19: Discharge, clogging, flow level, volume, and generated boulders in the Lower Debris Basin from one “normal” run, simulating the 2005 event.

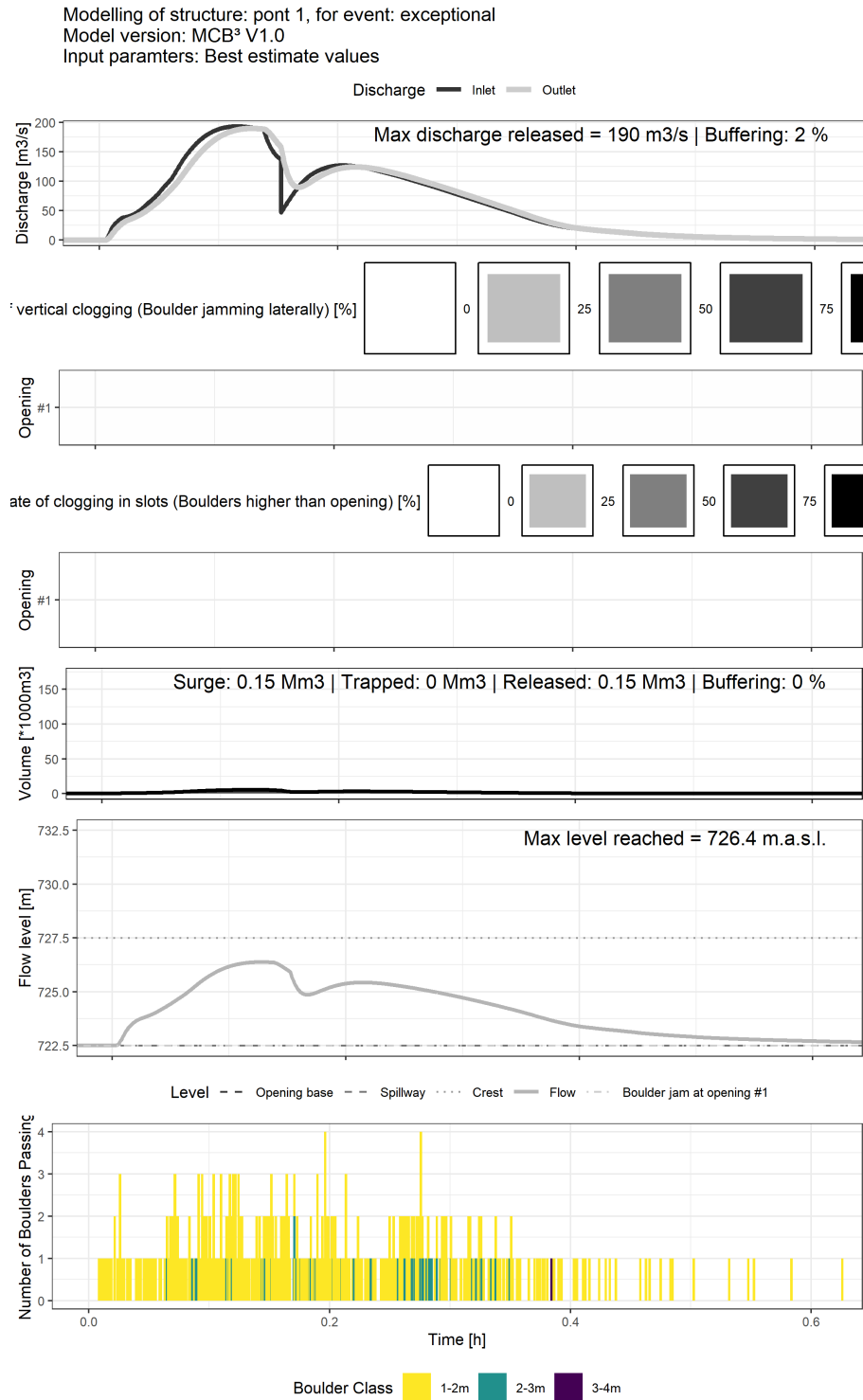


Figure 20: Discharge, clogging, flow level, volume, and generated boulders for the Lower Bridge from one “normal” run, simulating the 2005 event.

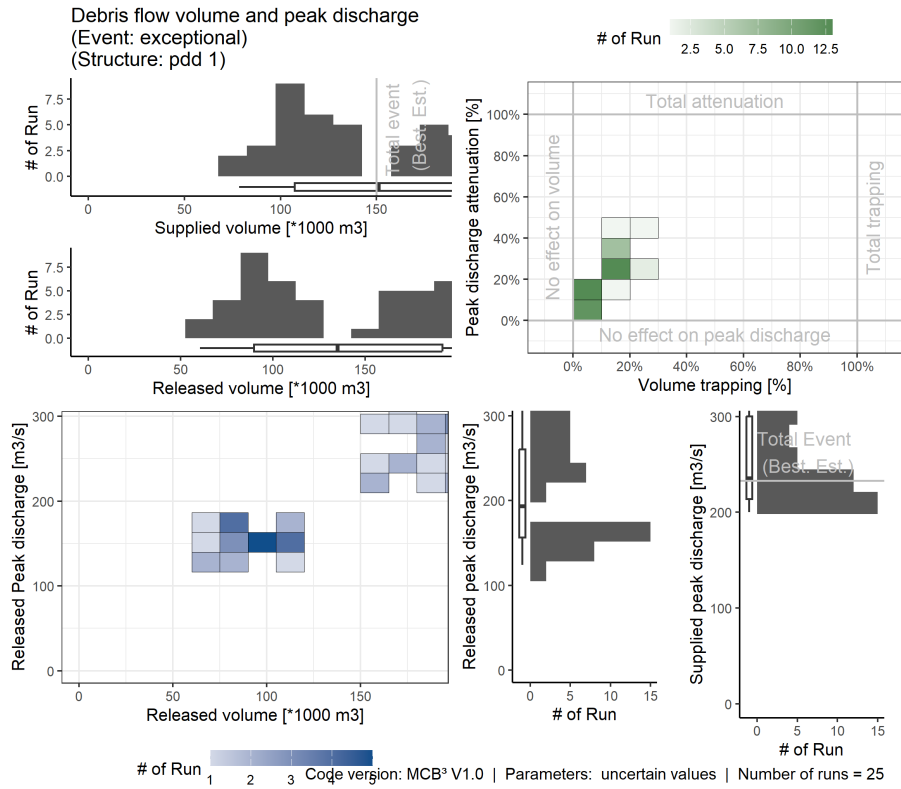


Figure 21: Results of the possibilistic analysis of the 2005 event, showing supplied volume, released volume, peak discharge, volume trapping, and attenuation within the Upper Debris Basin.

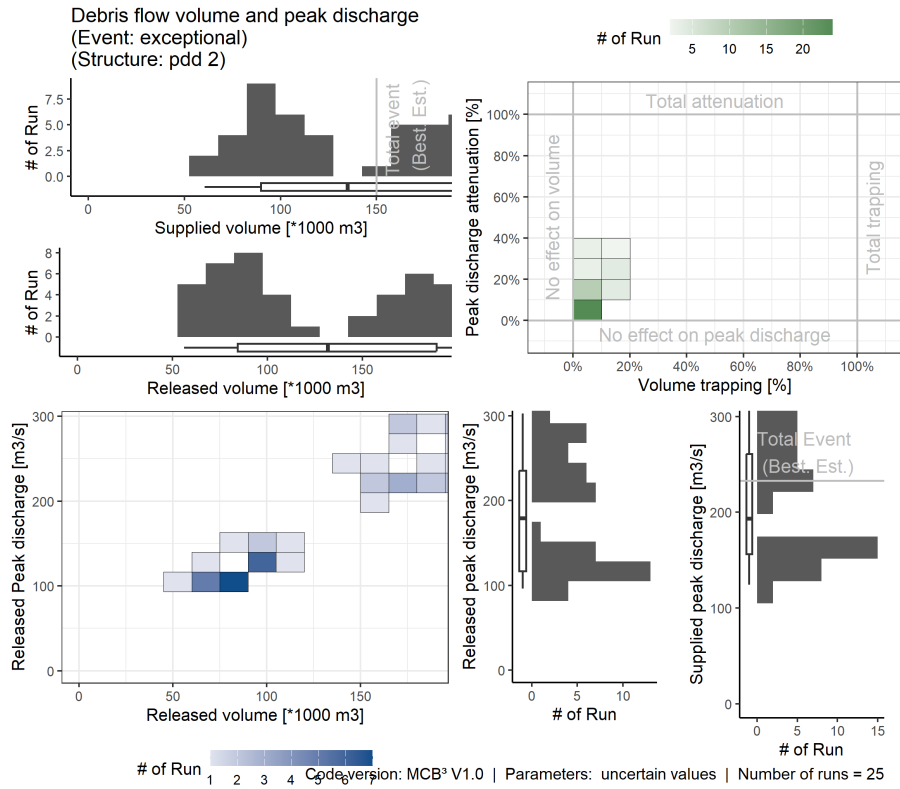


Figure 22: Results of the possibilistic analysis of the 2005 event, showing supplied volume, released volume, peak discharge, volume trapping, and attenuation within the Lower Debris Basin.

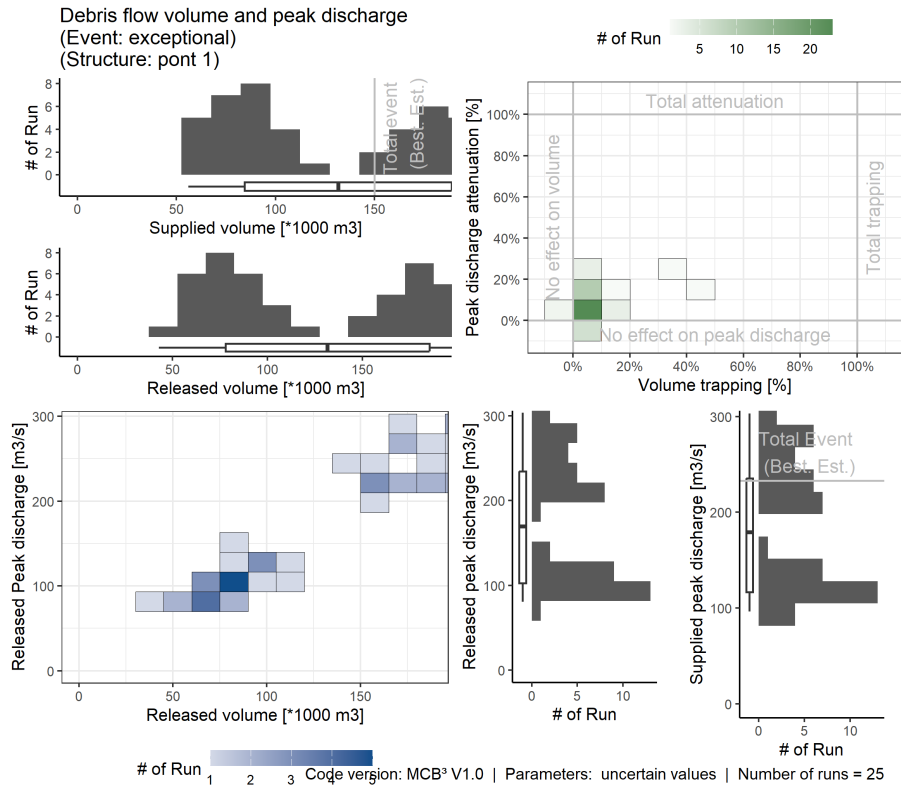


Figure 23: Results of the possibilistic analysis of the 2005 event, showing supplied volume, released volume, peak discharge, volume trapping, and attenuation upstream of the Upper Bridge.

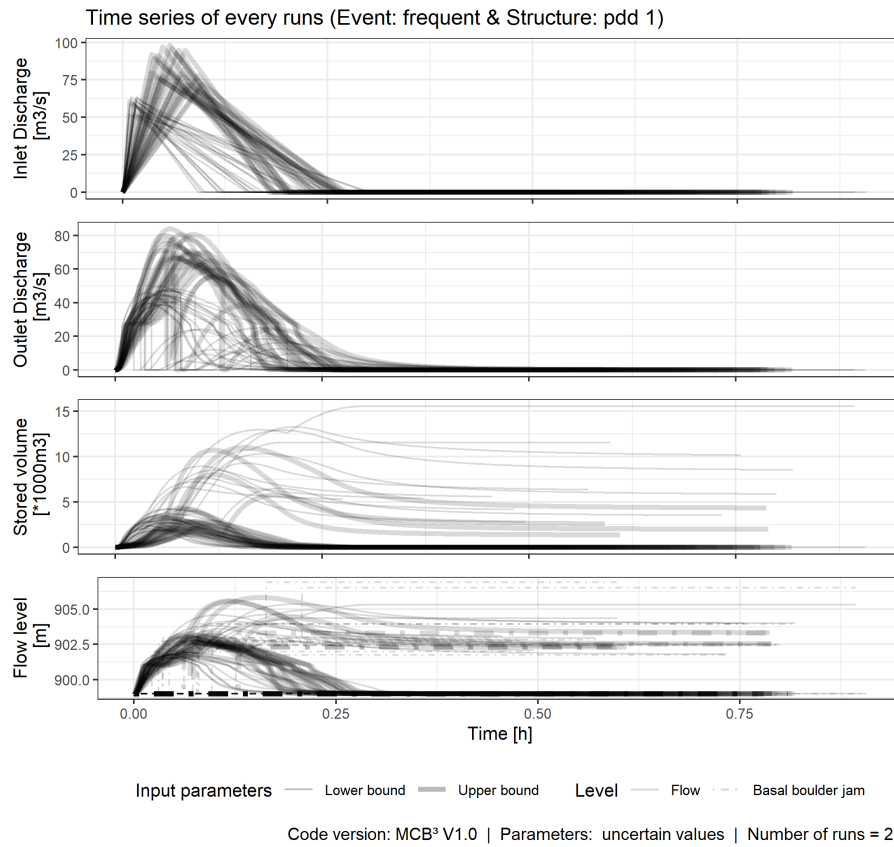


Figure 24: Results of the possibilistic analysis of the Frequent event (with a return period of approximately 10 years), showing supplied discharge, released discharge, stored volume, and flow level the the Upper Debris Basin.

F Limitations and Future Directions

There are several limitations to the model framework presented within this report, which may be addressed as part of future scopes of work. These limitations and future directions are outlined within this section.

Boulders are often concentrated at the front of a debris flow surge (Choi et al., 2016; Aaron et al., 2023), where the flow depth and shear stresses are greatest. While there are typically boulders present in the tail of the event, they are generally smaller and less concentrated (Aaron et al., 2023) (Figure 25). Currently, the model framework assumes that the probability of a boulder existing within a given packet is equal throughout the entire debris flow volume (Figure 25). This assumption is conservative, but maybe overly so. Users may consider truncating the debris flow hydrograph to simulate only the debris flow front, where boulders are most likely to be present. In this case, the simulation could be concluded once peak flow is reached (Figure 25). In future versions of the model, developers may revise the framework to account for a higher boulder concentration at the front of the surge, but this would require an additional input parameter, defining the increased concentration of boulders.

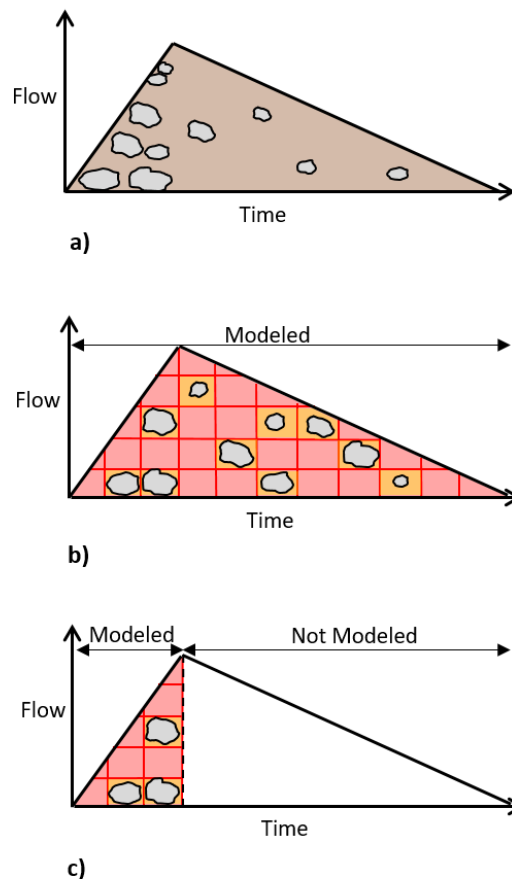


Figure 25: In debris flows, boulders are generally concentrated at the front of the surge (Choi et al., 2016; Aaron et al., 2023) (panel a). However, the current model framework assumes that boulders are equally likely to be present throughout the entire surge (panel b). This may be an overly conservative assumption. It is therefore proposed that in a future version of the model framework, the hydrograph is truncated after the peak flow is reached, to more realistically simulate the number and position of boulders within the surge (panel c).

The framework presented in this study does not include woody debris, which is often present in debris flows (Xie et al., 2023). Woody debris may cause jamming through constrictions (Wang et al., 2022b). Unlike boulders, woody debris jams tend to float on the surface of a debris flow, thereby causing deposition through hydraulic rather than mechanical control (Piton and Recking, 2016; Wang et al., 2022b). If the event volume is large enough to cause overtopping of a structure, the woody debris jam overtops as well (Horiguchi et al., 2021). With this release of woody debris, the hydraulic control is removed, potentially re-mobilizing sediment. Woody debris jams also sometimes burst, magnifying the amplitude of the debris flow (Chen et al., 2020; Wang et al., 2022a). As a debris flow event progresses, woody debris may be crushed by boulders, changing its size and therefore its probability of jamming (Rickli et al., 2018; Piton et al., 2024). Because of these factors, woody debris jams are difficult to predict and accurately model. Woody debris jamming was not included in the model framework presented within this report, but future research may focus on rectifying this gap.

The model framework presented in this study assumes that jamming is permanent, can only occur with one or two boulders, and is entirely dependent on the ratio of slit width to boulder diameter. This is a simplification of a complex physical process. Jamming may also occur when three or more particles form arches (Marchelli et al., 2020). While arches are sometimes stable, they also sometimes collapse (Marchelli et al., 2020; Choi et al., 2016; Zhou et al., 2020). Arches formed by compressible particles are more likely to collapse than those formed by rigid particles (Marchelli et al., 2020). Collapse also sometimes occurs due to collisional interactions with other particles. Arches are more likely to collapse in flows with high Froude numbers, as particle interactions tend to be more collisional (Choi et al., 2016) and to have higher velocities (Zhou et al., 2020). Future iterations of the modeling framework may consider modeling the formation and dissolution of arches.

Debris flows behave in a non-Newtonian manner (Xia and Tian, 2022; Hengbin Wu et al., 2015). The model framework presented in this study simulates flow through constrictions using the Slit Equation (Equation 1), Grand Orifice Equation (Equation 2), or the Weir Equation (Equation 3), all of which were developed assuming Newtonian, clear-water flow conditions. As far as we are aware, there has been no research into whether these equations are applicable to non-Newtonian processes such as debris flows. With no scientific evidence to either contradict or support the use of these equations within the model framework, they are assumed reasonable for the purposes of this analysis. If research in this area is published, this assumption may be revisited for future iterations of the framework.

The model framework assumes that all boulders that are not jammed are transferred to the downstream structure, i.e. none of the debris flow volume stored behind a jam is composed of boulders. If instantaneous transfer is selected, then the previously generated boulders are routed directly to the downstream structure. If mixing transfer is selected, the boulders are stochastically regenerated within the mixing volume from the number of boulders that pass through the upstream structure. This assumes that all the deposition and re-entrainment causing mixing occurs from within the debris flow volume, and the overall probability of boulders is conserved between structures. These assumptions do not completely reflect the nuanced reality of a debris flow event. Boulders along with mud may be deposited upstream of a constriction. As well, boulders resting within the channel (for example from previous debris flow events, or from insufficiently sized riprap) may be entrained between structures, increasing the overall number of boulders within the event. While this limitation is likely partially accounted for by the possibilistic nature of the analysis, we recommend that practitioners keep it in mind when selecting the upper and lower bounds for boulder number prior to simulations.



Centre Center Lyon-Grenoble - Auvergne-Rhône-Alpes
2 rue de la Papeterie BP 76,
38 402 St-Martin-d'Hères - France

Rejoignez-nous sur :



<https://www.inrae.fr/centres/lyon-grenoble-auvergne-rhone-alpes>



**RÉPUBLIQUE
FRANÇAISE**

*Liberté
Égalité
Fraternité*

INRAE